

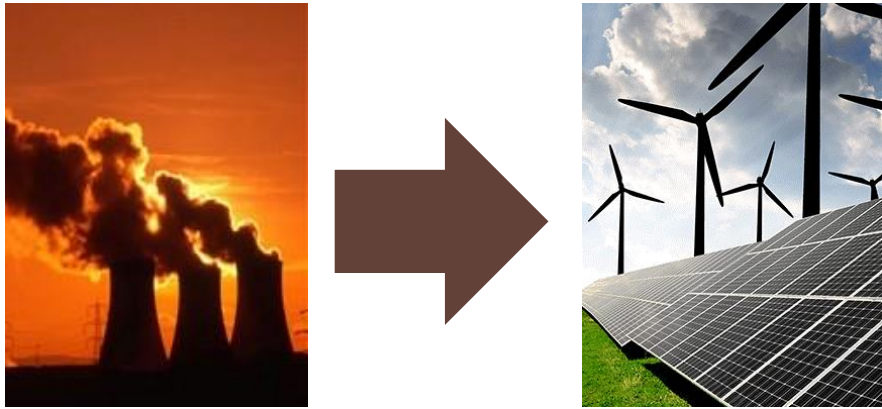
Dynamic Estimation and Control of Power System

Prof. Bikash C. Pal

Control and Power Group
Electrical and Electronic Engineering
Imperial College London

Introduction

- Transition to low-carbon generation



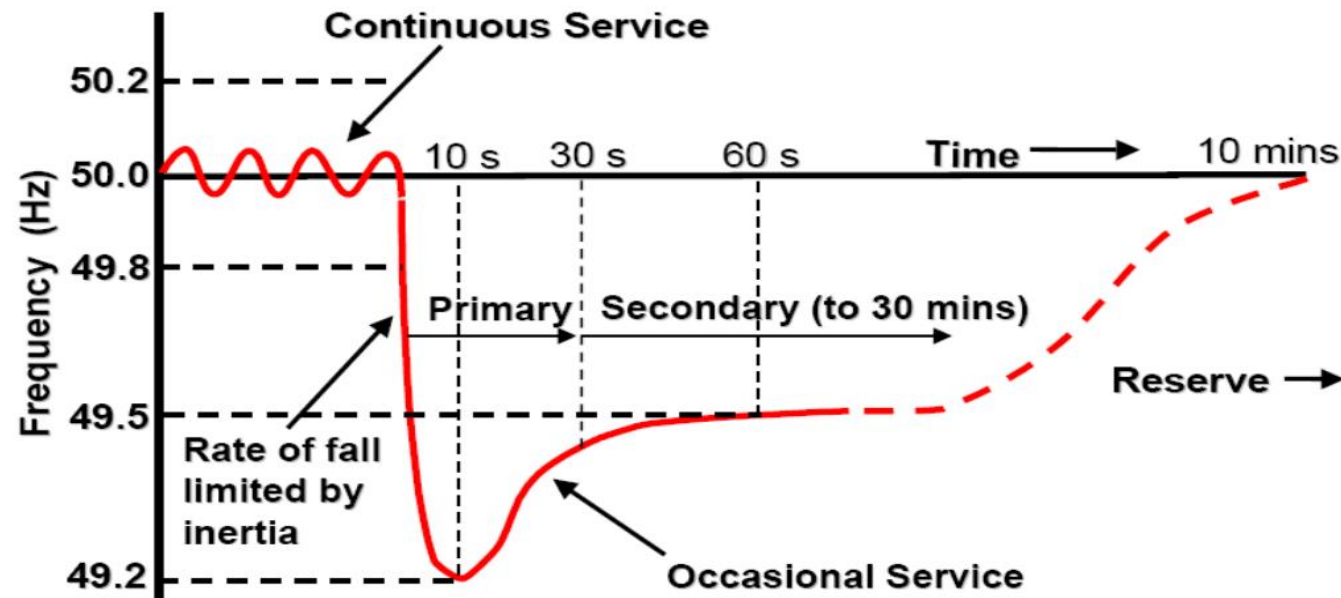
- New operation and generation challenge
 - Reduced system inertia
 - System characteristics and operating status change dynamically and unpredictably
 - Uncertainty in model - reduced observability and controllability
 - Real-time estimation of system status is now crucial

Why dynamic state estimation?

The need for real-time estimation of system operating status is satisfied using dynamic state estimation

- States which describe oscillatory dynamics of the system, such as power angle, equivalent rotor speed, transient fluxes and voltages, are estimated dynamically
- These dynamic states can be used to design controllers for power plants, or for FACTS devices such as STATCOMs and TCSCs
- Can be used for system control and protection following small and large disturbances

Requirements for DSE



- Estimation should work for continuous-service periods as well as for the transient and occasional-service periods
- Estimation model should be detailed enough to consider all the factors which affect the states during the transient period
- The time delay for estimating the states should be as low as possible

Challenges to centralized dynamic state estimation

- The update-rates of the communication networks used in present day power systems not fast enough
- Real-time knowledge of system-wide model and operating condition is required
- Communication packet dropouts, random time delays, packet disordering and cyber-security threats need to be addressed

Alternative: Decentralization

- Decentralization is the most logical alternative to centralized estimation and control as it effectively eliminates each one of its challenges
- How to decentralize when each component of power system is strongly coupled to the rest of the system?
- For example, all the generation units (or machines) are coupled to each other and to the rest of the network through differential and algebraic equations (DAEs):

$$\dot{\mathbf{x}}_c(t) = \mathbf{g}(\mathbf{x}_c(t), \mathbf{u}_c(t), \mathbf{y}_c(t)); \mathbf{y}_c(t) = \mathbf{h}(\mathbf{x}_c(t), \mathbf{u}_c(t))$$
$$\Rightarrow \dot{\mathbf{x}}_c(t) = \mathbf{g}(\mathbf{x}_c(t), \mathbf{u}_c(t), \mathbf{h}(\mathbf{x}_c(t), \mathbf{u}_c(t)))$$

Decentralization using 'pseudo-inputs'

- These DAEs are decoupled if the terminal voltage and phase (V, θ) are treated as inputs, and node current and its phase (I, ϕ) are treated as normal measurements.

$$x_{ci} = [\delta_i \ \omega_i \ E'_{di} \ E'_{qi} \ \psi_{1di} \ \psi_{2qi} \ E'_{dci} \ V_{ri}]^T, \ u_{ci} = V_{ssi},$$
$$u'_{ci} = [V_{ui} \ \theta_{ui}]^T; \ \dot{x}_{ci}(t) = g_i(x_{ci}(t), u_{ci}(t), u'_{ci}(t))$$

- This is done by subtracting noise (V_w, θ_w) from (V, θ):

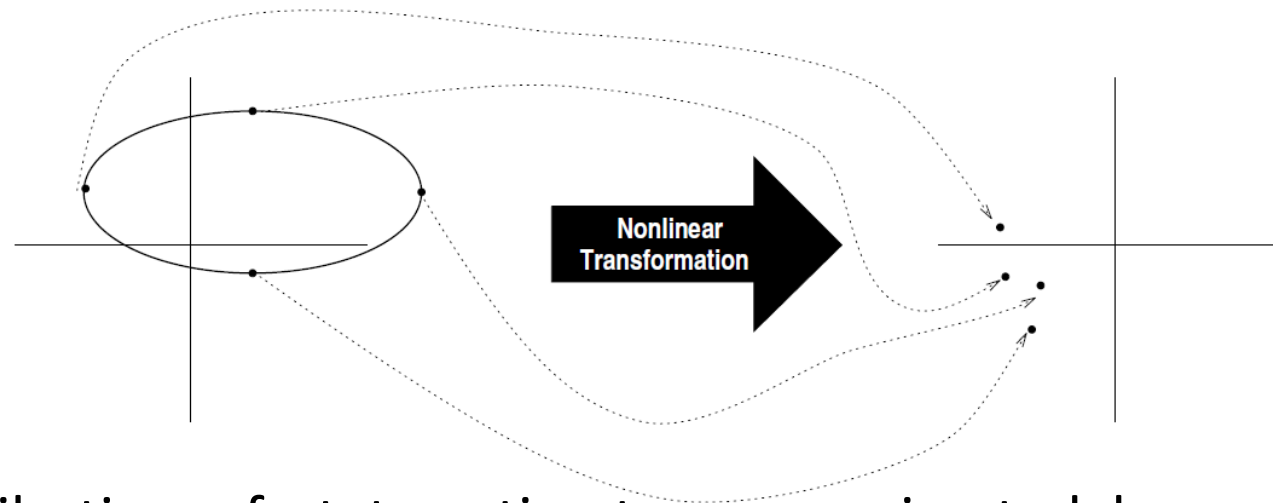
$$V_u = V - V_w, \quad \theta_u = \theta - \theta_w$$

- The pseudo-inputs (V_u, θ_u) make the estimation and control for one unit completely independent of the other units

Decentralized dynamic state estimation

- As node voltage & current phasor pairs, (V, θ) and (I, ϕ) , are algebraic electromagnetic quantities, any change/disturbance in the system is instantaneously reflected in voltage & current phasors of all the nodes in the system.
- Hence, by decoupling the system equations by treating one pair of (V, θ) and (I, ϕ) as input while other as output (or normal measurement), we are not losing any information in the decoupled equations for one generating unit.
- If the decoupled equations are used in a non-linear filtering technique, such as unscented Kalman filtering (UKF) or extended particle filtering (EPF), then dynamic state estimation (DSE) for a power system becomes completely decentralized.
- Decentralized DSE uses locally available parameters and measurements at a machine, and provides all the dynamic states of the machine in real-time

Unscented Kalman filtering (UKF)



- Probability distribution of state-estimates approximated by generating ‘sigma points’, instead of linearization.
- Thus, non-linearity in the state equations is preserved, and costly linearization is avoided.
- V_w and ϑ_w are assumed to be white noises; and are treated as states in the filtering equations.
- l and ϕ are treated as normal measurements.

Generation of sigma points

$$\chi_{il}(k) = \hat{X}_i(k-1) + \left(\sqrt{n_i P_{X_i}(k-1)} \right)_l ; l = 1, 2, \dots, n_i$$

$$\chi_{il}(k) = \hat{X}_i(k-1) - \left(\sqrt{n_i P_{X_i}(k-1)} \right)_l ; l = 1 + n_i, 2 + n_i, \dots, 2n_i$$

- Here χ_{il} is the l^{th} sigma point for the i^{th} generating unit.
- $\left(\sqrt{n_i P_{X_i}(k-1)} \right)_l$ is the l^{th} column of $\sqrt{n_i P_{X_i}(k-1)}$, which is found by Cholesky factorization of $n_i P_{X_i}(k-1)$.
- X_i is state vector of the i^{th} unit, \hat{X}_i is its estimated mean, P_{X_i} is its covariance and number of elements in it is n_i .

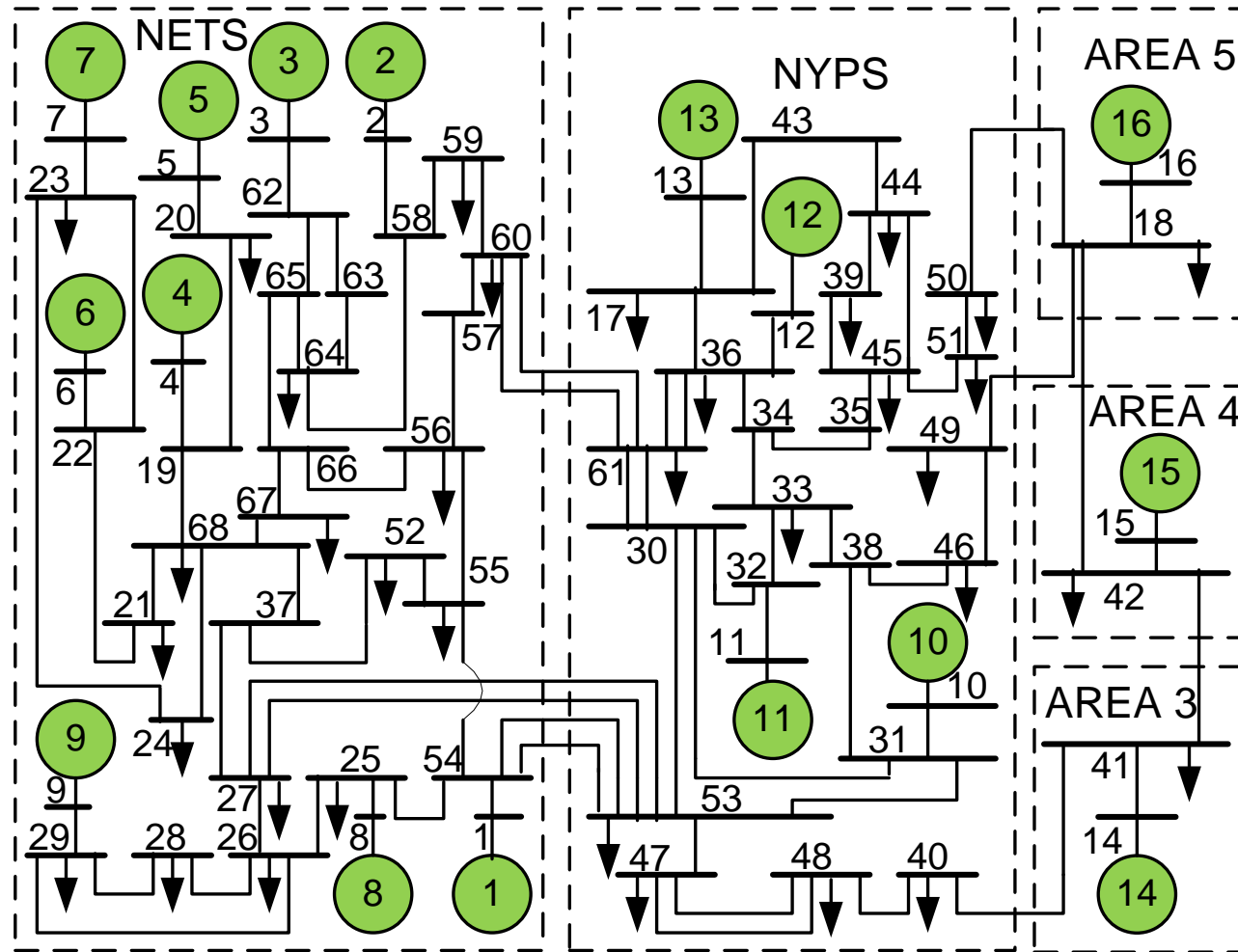
UKF filtering equations for the k^{th} sample

- State prediction: $\chi_{il}^- = g_i[\chi_{il}, u_i']$; $l = 1, 2, \dots, 2n_i$
 $\hat{X}_i^- = \text{mean of } \chi_{il}^-$, $P_{X_i}^- = \text{covariance of } \chi_{il}^- + \text{process noise}$
- Measurement prediction: $\gamma_{il}^- = h_i[\chi_{il}^-, u_i']$; $l = 1, 2, \dots, 2n_i$ $\hat{y}_i^- = \text{mean of } \gamma_{il}^-$, $P_{y_i}^- = \text{covariance of } \gamma_{il}^- + \text{measurement noise}$, $P_{X_i y_i}^- = \text{cross-covariance of } \chi_{il}^- \text{ and } \gamma_{il}^-$
- Kalman update: $K = P_{X_i y_i}^- (P_{y_i}^-)^{-1}$, $\hat{X}_i = \hat{X}_i^- + K(y_i - \hat{y}_i^-)$, $P_{X_i} = P_{X_i}^- - K(P_{X_i y_i}^-)^T$

Noise model

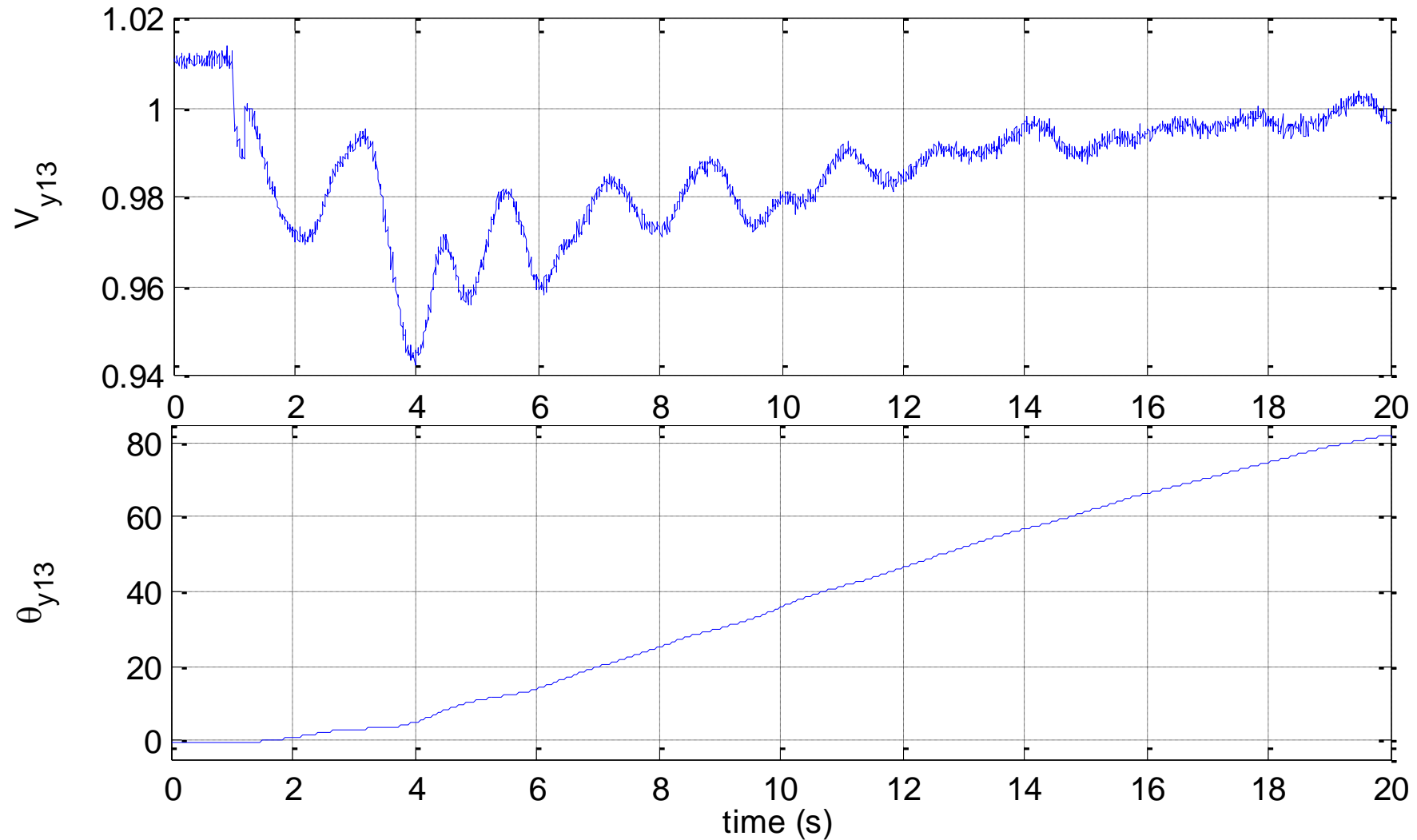
- Measurement noise: V_w (noise in voltage magnitude), I_w (in current magnitude), θ_w (in voltage phase) and ϕ_w (in current phase) taken as white Gaussian noises.
- Total vector error (TVE) in V_w and θ_w , and I_w and ϕ_w is taken as 1% (as per IEEE C37.118.1-2014a standard for PMUs)
- Process noise: Random noise of known variance (and of similar order as measurement noise variances) added to the simulated power system model in order to account for process noise. In practice, process noise variances are estimated using a perturbation observer.

Test system: 68-bus benchmark system

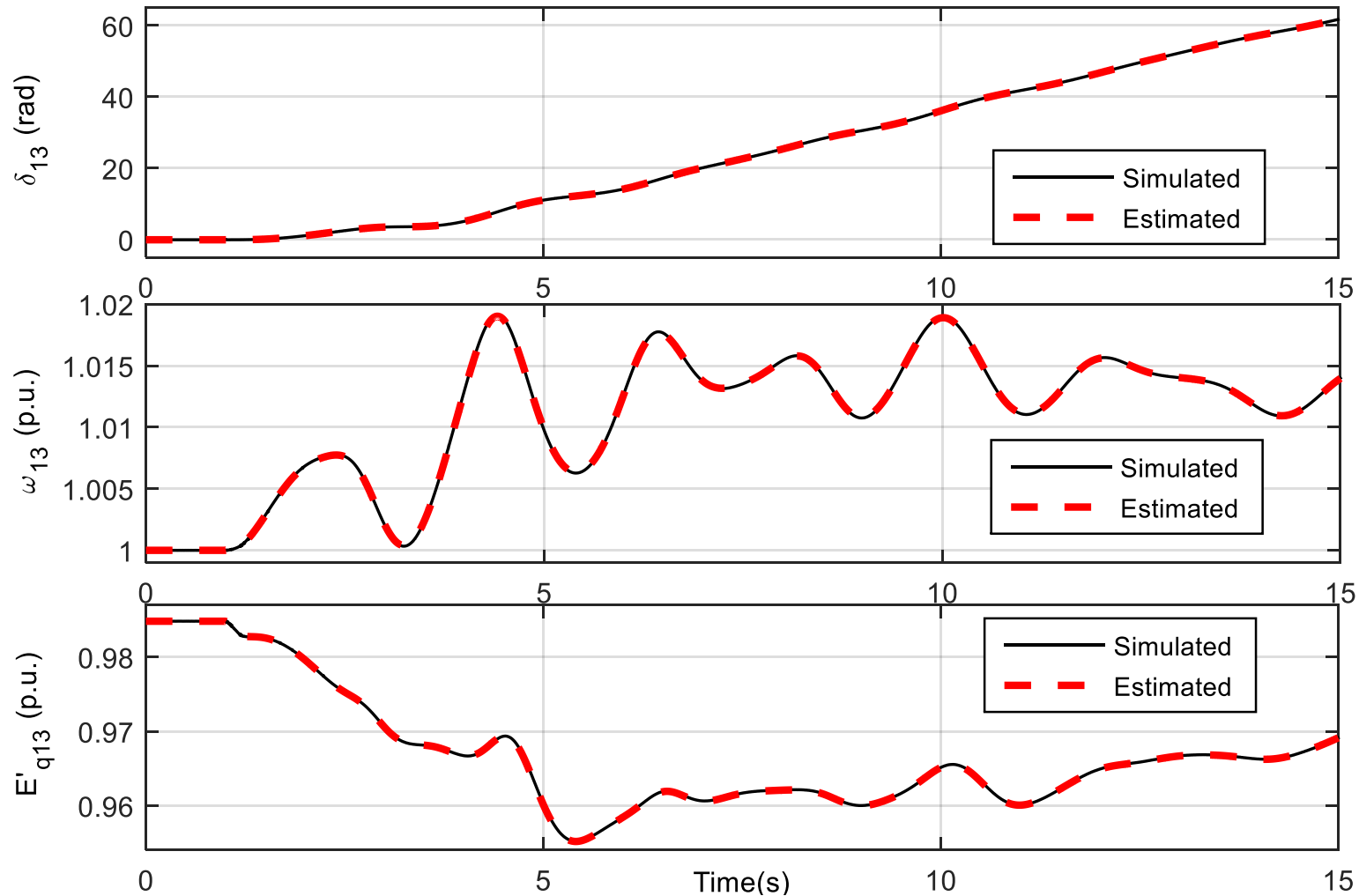


Sub-transient dynamic model used for all the machines

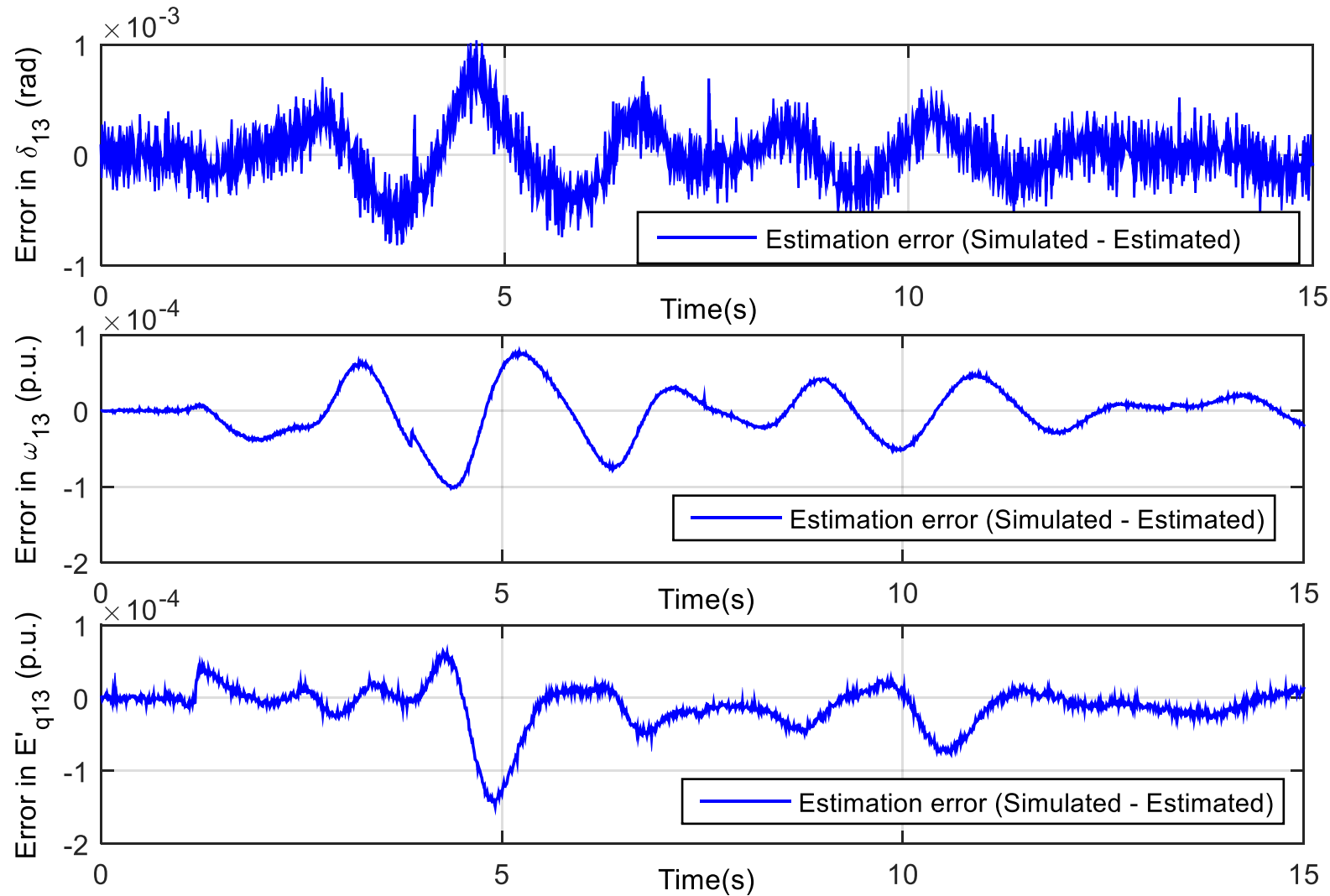
Generated measurements



Results: estimation accuracy



Estimation accuracy (cont.)



Computational feasibility

	Average computational time for one iteration (in ms)	
Test system	Decentralized algorithm	Centralized algorithm
IEEE 30-bus	0.33	1.45
IEEE 68-bus	0.33	12.4
IEEE 145-bus	0.33	139

Bad-data detection

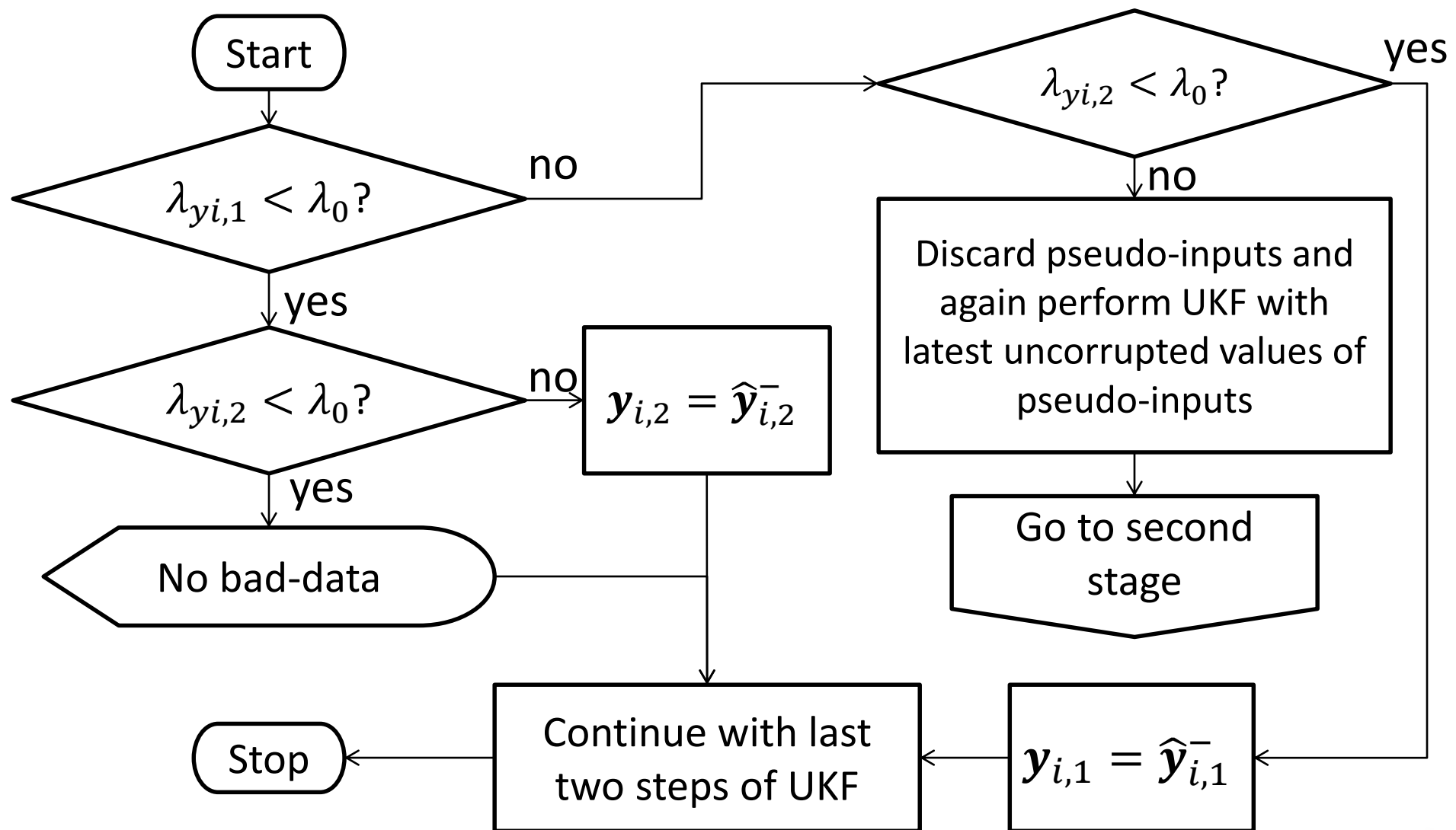
- Two stage algorithm, as bad-data can be present in either measurements, or pseudo-inputs or both.
- Condition for absence of bad data:

$$\lambda_{yi,1} < \lambda_0, \text{ where } \lambda_{yi,1} = |\mathbf{y}_{i,1} - \hat{\mathbf{y}}_{i,1}^-| / \sqrt{\mathbf{P}_{y_{i,1}}^-}$$

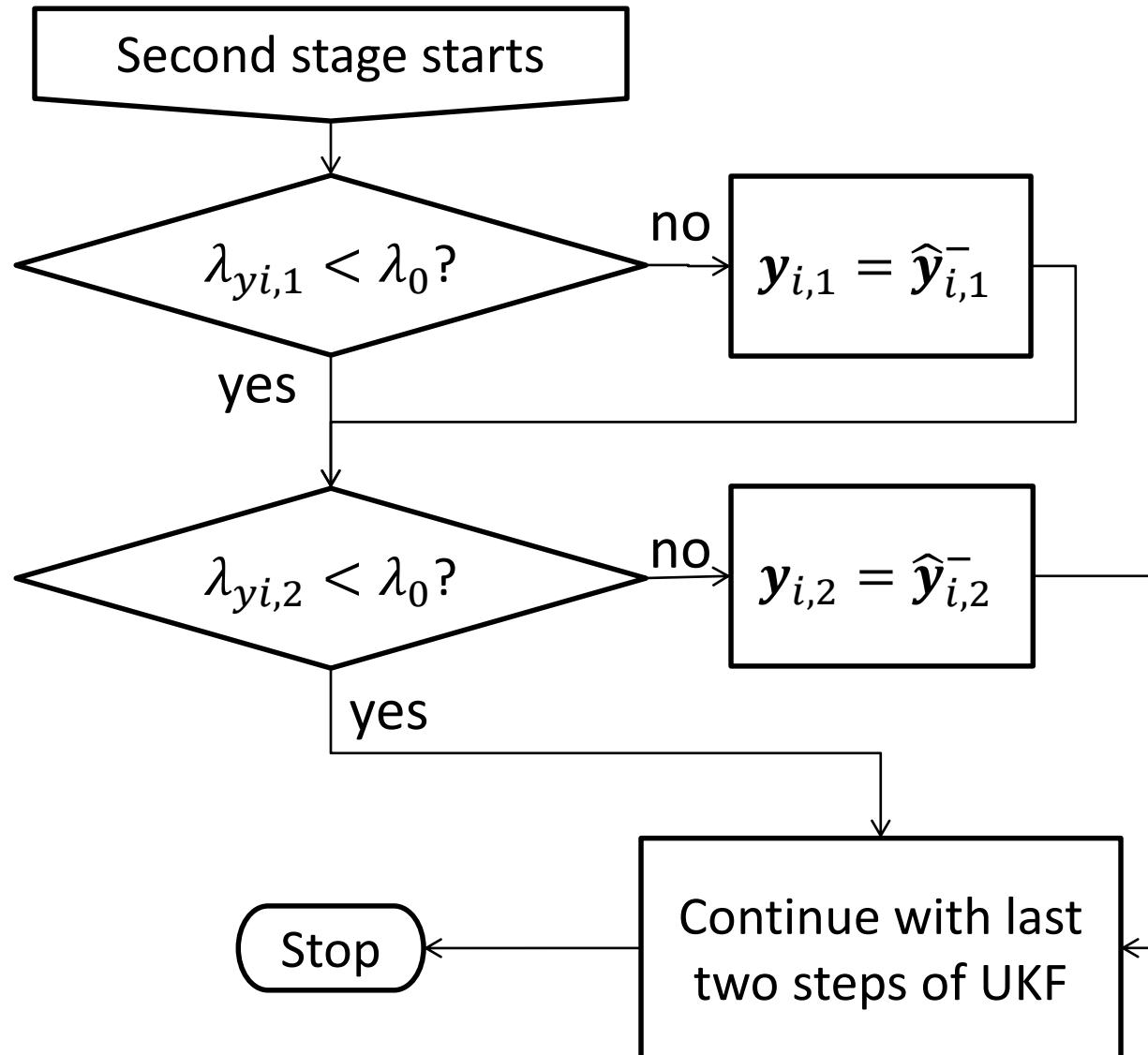
$$\text{and } \lambda_{yi,2} < \lambda_0, \text{ where } \lambda_{yi,2} = |\mathbf{y}_{i,2} - \hat{\mathbf{y}}_{i,2}^-| / \sqrt{\mathbf{P}_{y_{i,2}}^-}$$

- Here, $\mathbf{y}_i = [\mathbf{y}_{i,1}, \mathbf{y}_{i,2}]^T$, $\hat{\mathbf{y}}_i^- = [\hat{\mathbf{y}}_{i,1}^-, \hat{\mathbf{y}}_{i,2}^-]^T$, and $[\mathbf{P}_{y_{i,1}}^-, \mathbf{P}_{y_{i,2}}^-]$ are diagonal elements of $\mathbf{P}_{y_i}^-$
- λ_0 depends on system (= 10 for case system)

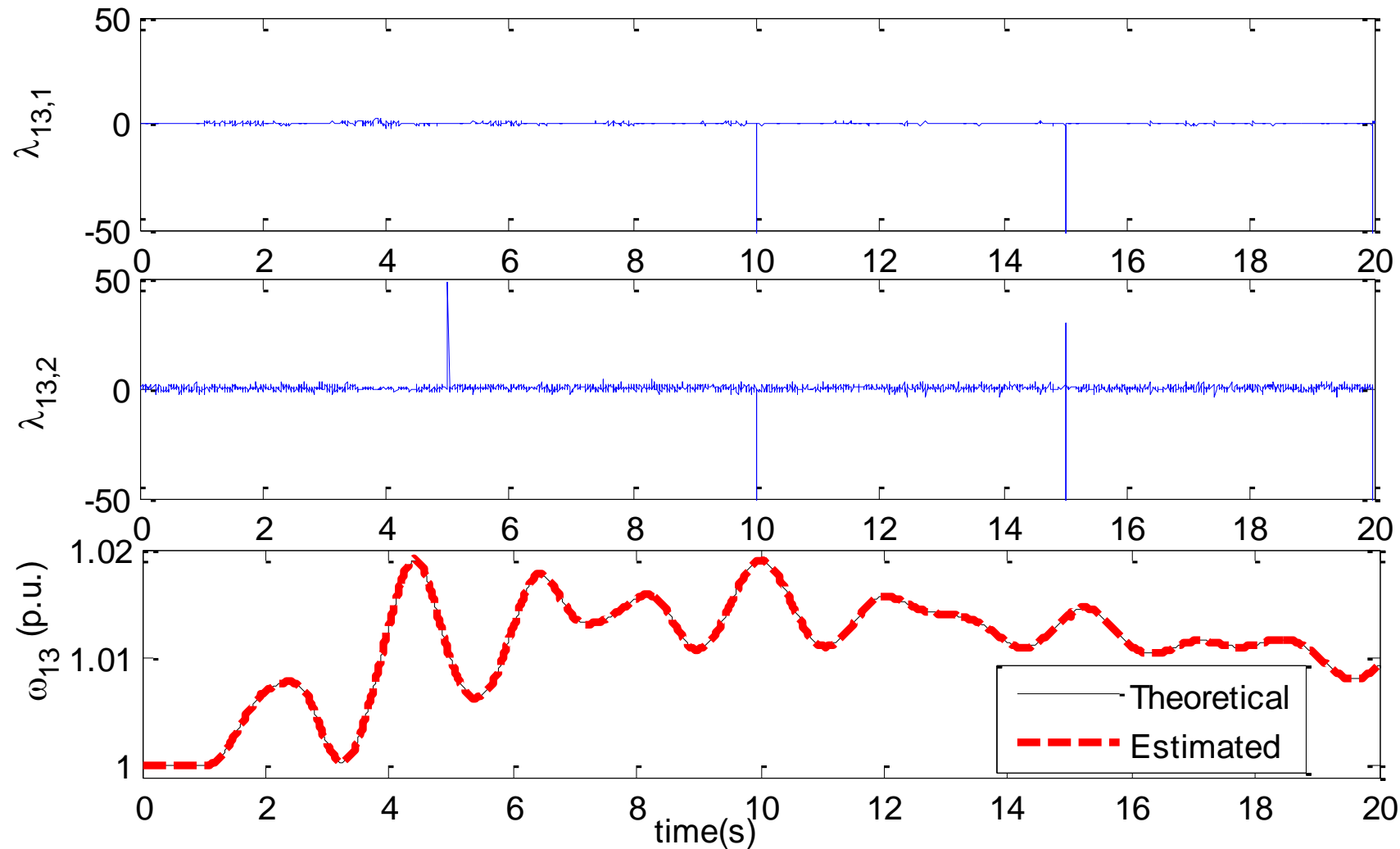
Bad-data detection flow chart: first stage



Flow chart: second stage



Bad-data detection (spikes show bad data)



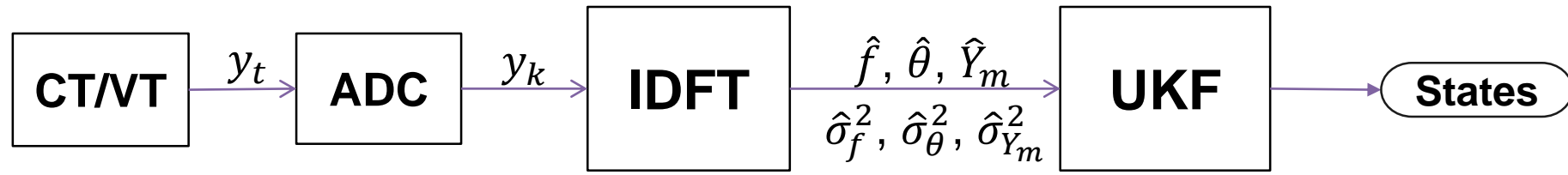
Drawbacks of PMU based DSE

- PMUs rely on GPS synchronization
- GPS susceptible to atmospheric effects, clock errors and multipath effects
- Issue of cyber-security
- Poor accuracy for standard PMU-noise
- Vendor dependent accuracy, latency and sampling rate

Finding alternative to PMU based DSE

- Through GPS synchronization, PMUs provide a common reference frame for obtaining voltage and current phasors, and these phasors are required for DSE
- Errors in GPU synchronization translate to errors in phasor measurements, which then translate to errors in DSE
- Reliance on GPS synchronization can be removed if we remove the requirement of a common reference frame in the estimation model
- This can be done if we estimate 'internal angle' α , instead of rotor angle δ , as $\alpha = \delta - \theta$, and being a *relative angle*, α does not require a reference frame
- Dynamic equation of α is: $\dot{\alpha} = \omega - f$. Rest of the states and dynamic equations remain same as PMU-based DSE.
- As frequency f is used instead of θ , the new pseudo inputs are (V, f) .
- δ can be obtained after performing DSE using $\delta = \alpha + \theta$ (provided θ is available)

Robust two stage DSE using IDFT and UKF



- Analog signals of voltage and current from CT and VT are sampled at very high rate (40kHz)
- IDFT stage: Frequency (f), phase (θ) and magnitude (Y_m) calculated as parameters of the analog signal samples y_k using interpolated discrete-time Fourier transform (IDFT)
- UKF stage: Estimated mean and variances of these parameters (f , θ and/or Y_m) are used to find estimates of states using unscented Kalman filter (UKF)

IDFT stage

- If N samples of a signal are multiplied with N samples of Hann window function, $h_k = \sin^2\left(\frac{\pi k}{N}\right)$, and the DFT of the product is found, denoted by Z_λ , $\lambda \in \{0, 1, \dots, (N-1)\}$, with f_s as the sampling frequency, then \hat{f} , $\hat{\theta}$ and \hat{Y}_m are:

$$\hat{f} = \sqrt{\frac{Z_0 + 2Z_1 + 9Z_2}{Z_0 - 2Z_1 + Z_2}}, \hat{\theta} = \frac{1}{2j} \ln \left\{ \frac{Z_0 F - Z_1 C}{Z_1 B - Z_0 E} \right\}, \hat{Y}_m = \frac{8\pi Z_0 / N}{B e^{j\hat{\theta}} + C e^{-j\hat{\theta}}}$$

$$B = \frac{1 - e^{j2\pi\hat{f}N/f_s}}{\frac{\hat{f}N}{f_s} - \left(\frac{\hat{f}N}{f_s}\right)^3}, C = \frac{1 - e^{-j2\pi\hat{f}N/f_s}}{\frac{\hat{f}N}{f_s} - \left(\frac{\hat{f}N}{f_s}\right)^3}, E = \frac{1 - e^{j2\pi\hat{f}N/f_s}}{\frac{\hat{f}N}{f_s} - 1 - \left(\frac{\hat{f}N}{f_s} - 1\right)^3}, F = \frac{1 - e^{-j2\pi\hat{f}N/f_s}}{\frac{\hat{f}N}{f_s} + 1 - \left(\frac{\hat{f}N}{f_s} + 1\right)^3}$$

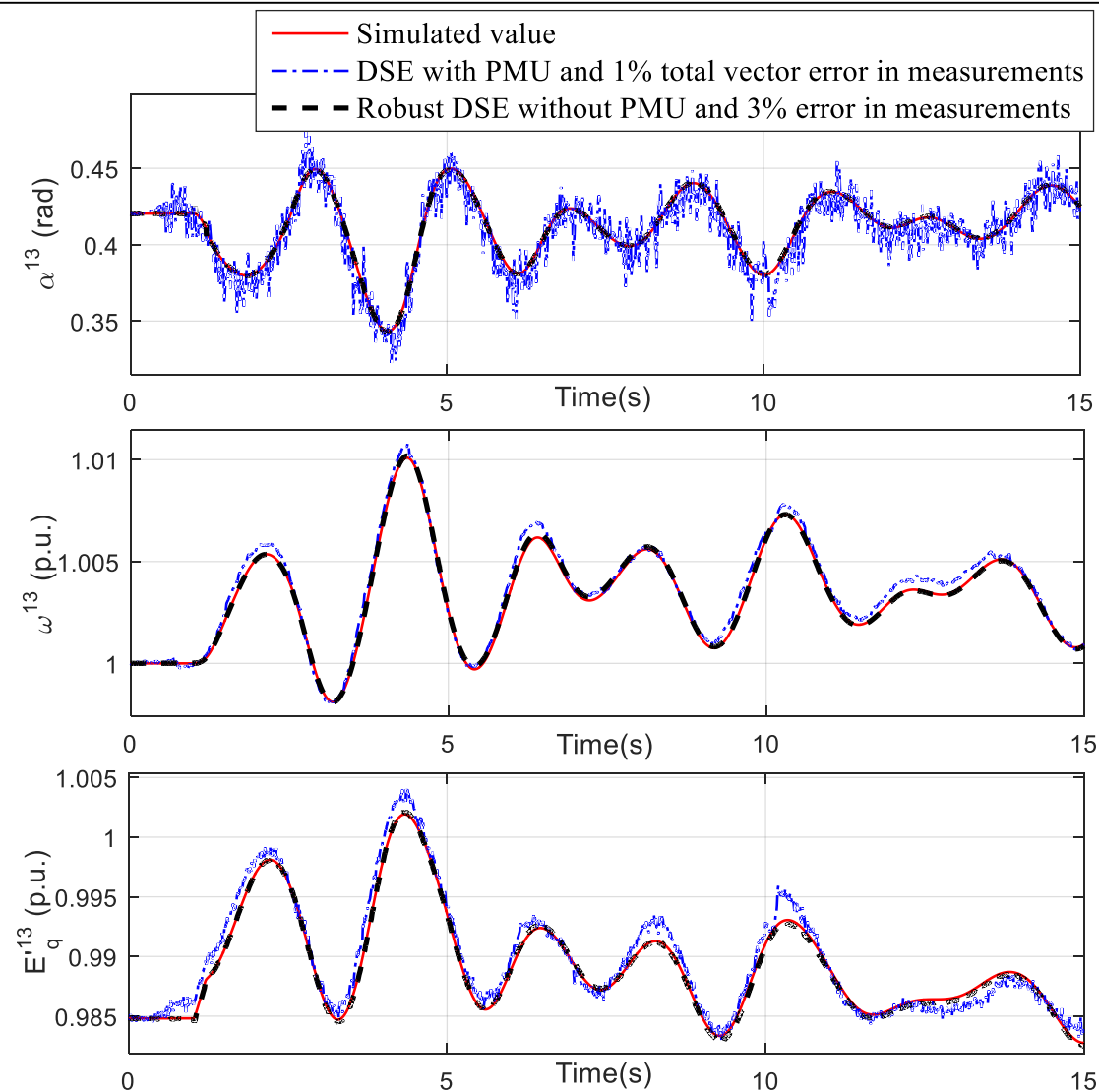
- Variances of \hat{f} , $\hat{\theta}$ and \hat{Y}_m , denoted by $\hat{\sigma}_f^2$, $\hat{\sigma}_\theta^2$ and $\hat{\sigma}_{Y_m}^2$, in terms of the variance of the noise in the signal, $\hat{\sigma}_y^2$, are:

$$\hat{\sigma}_f^2 = \left(\frac{f_s}{2\pi}\right)^2 \frac{48\hat{\sigma}_y^2}{\hat{Y}_m^2 N(N^2-1)}, \hat{\sigma}_\theta^2 = \frac{24\hat{\sigma}_y^2(2N+1)}{\hat{Y}_m^2 N(N-1)}, \hat{\sigma}_{Y_m}^2 = \frac{4\hat{\sigma}_y^2}{N}$$

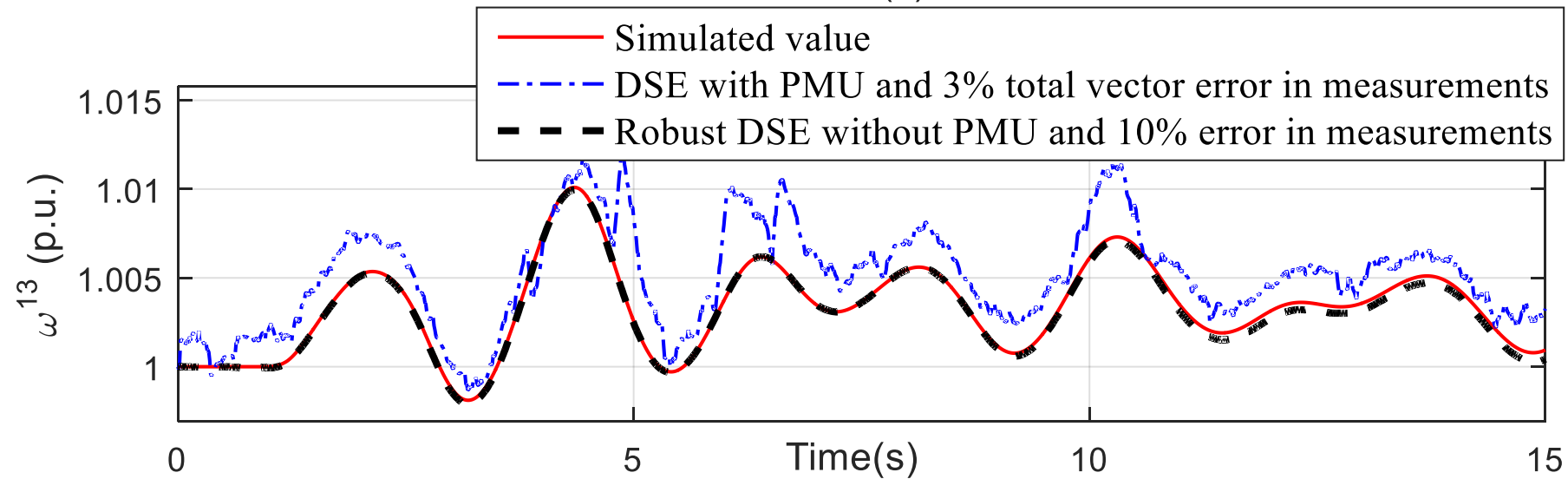
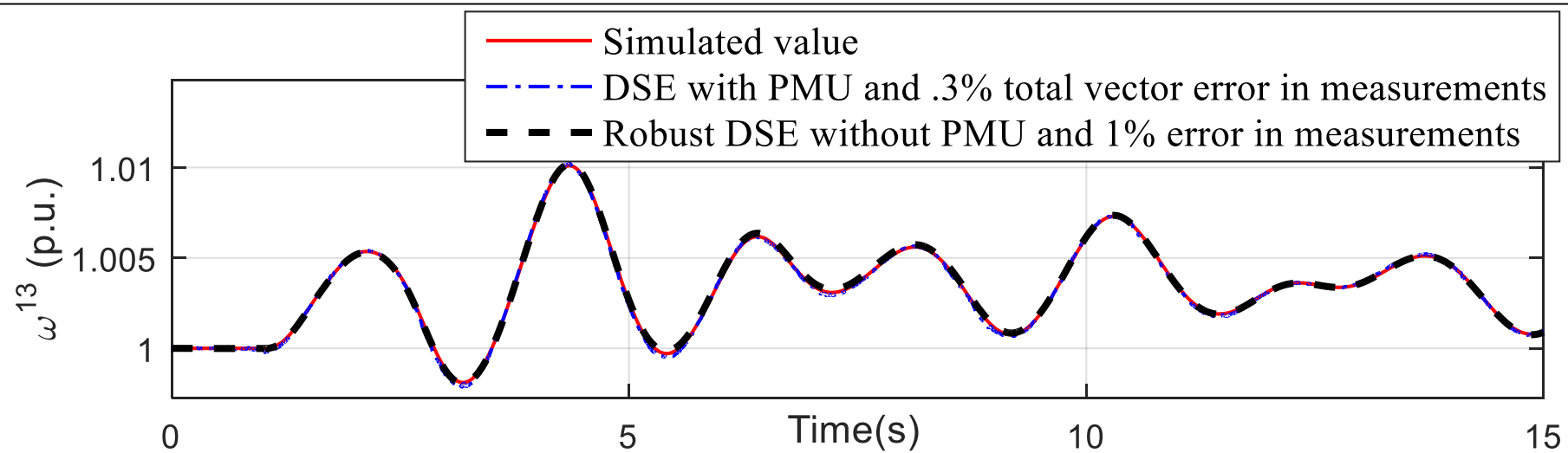
UKF stage

- \hat{f} , \hat{Y}_m , $\hat{\sigma}_f^2$, and $\hat{\sigma}_{Y_m}^2$, obtained for analogue V and I , are given as inputs to the second stage, and the four steps of unscented Kalman filtering are applied to recursively obtain the final estimate \hat{X}_k and its covariance P_k
- In case of Robust-DSE, \hat{X} is $[\hat{\alpha}_i \ \hat{\omega}_i \ \hat{E}'_{di} \ \hat{E}'_{qi} \ \hat{\psi}_{1di} \ \hat{\psi}_{2qi} \ \hat{V}_{ri}]^T$
- Because of constant updation of variances of V and I , the obtained estimates remain accurate for varying operating scenarios – another reason behind robustness (besides removal of reference frame)

Results of robust dynamic state estimation



Results of DSE: Effect of error in measurements



Results: Comparison of DSE estimation errors

State	RMSE (p.u.) for DSE-with-PMU and 1% TVE	RMSE (p.u.) for Robust DSE and 3% M. Error
Rotor angle ($\hat{\delta}_{13}$)	7.2×10^{-3}	5.9×10^{-4}
Rotor speed ($\hat{\omega}_{13}$)	4.1×10^{-4}	7.8×10^{-5}
Transient EMF for d-axis (\hat{E}'_{d13})	1.2×10^{-3}	1.8×10^{-4}
Transient EMF for q-axis (\hat{E}'_{q13})	1.9×10^{-3}	3.3×10^{-4}
Sub-transient EMF for d-axis ($\hat{\psi}_{1d13}$)	2.8×10^{-3}	4.2×10^{-4}
Sub-transient EMF for q-axis ($\hat{\psi}_{2q13}$)	2.2×10^{-3}	4.3×10^{-4}
AVR state (\hat{V}_{r13})	1.6×10^{-2}	4.5×10^{-3}

Benefits of robust DSE

- An assumption free, robust estimation method, which takes care of all the changes taking place in the system
- Local CT/VT measurements, hence not affected by GPS, or non-standard accuracy, latency or sampling rates of PMUs
- Dual stage estimation method filters noise, harmonics, bad-data and improves results with each new measurement
- Estimation process remains valid for any state of operation – steady state operation or transient operation
- Low estimation time delay: 40 ms

Extension of the decentralization-idea to dynamic parameter estimation

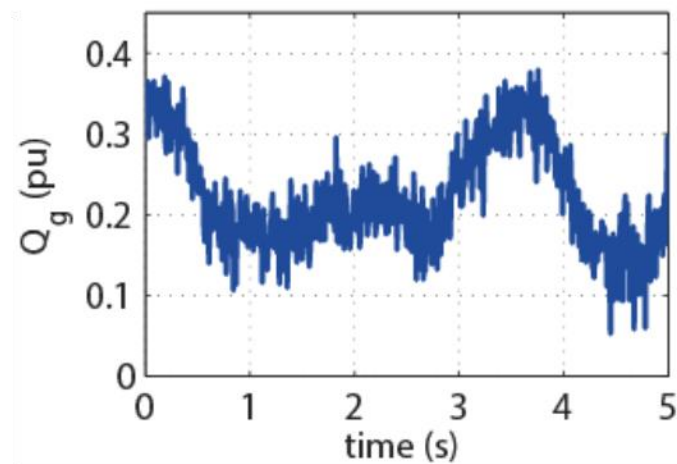
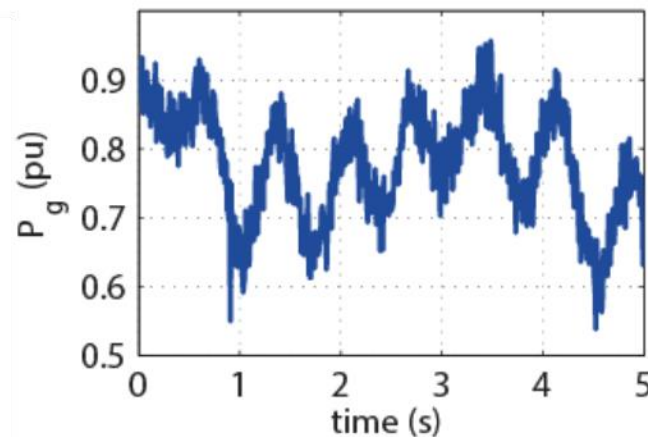
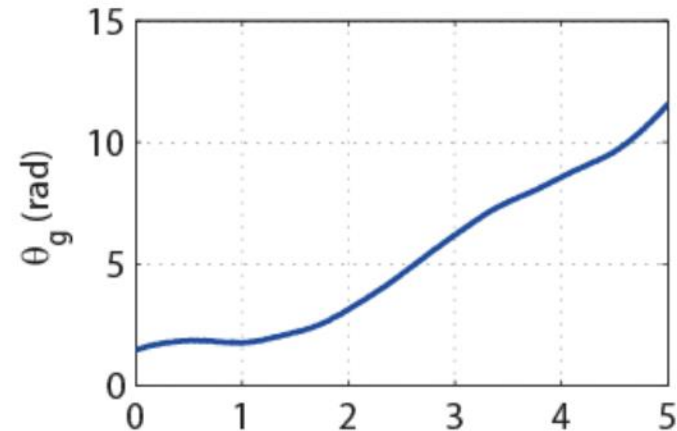
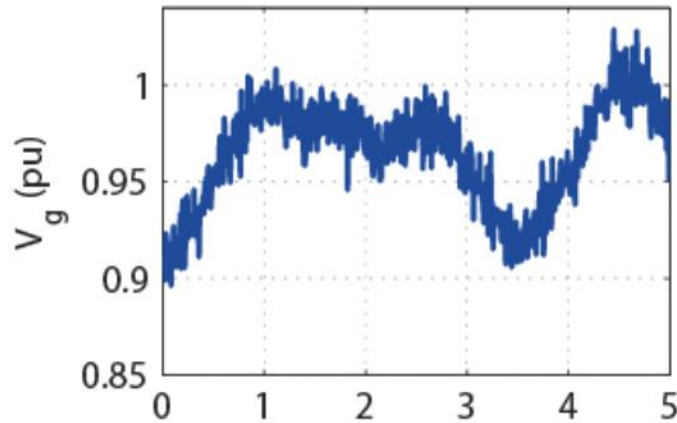
- The setting of an out-of-step relay is primarily dictated by three parameters:
 - Direct axis transient reactance, x'_d ,
 - Quadrature axis speed voltage, E_q , and
 - Generator inertia, H
- These parameters can change:
 - Due to operational changes and during oscillations
 - Due to addition of renewable generation at transmission level
- Thus, the relay settings should be updated regularly by dynamically estimating these parameters

Dynamic parameter estimation: Steps

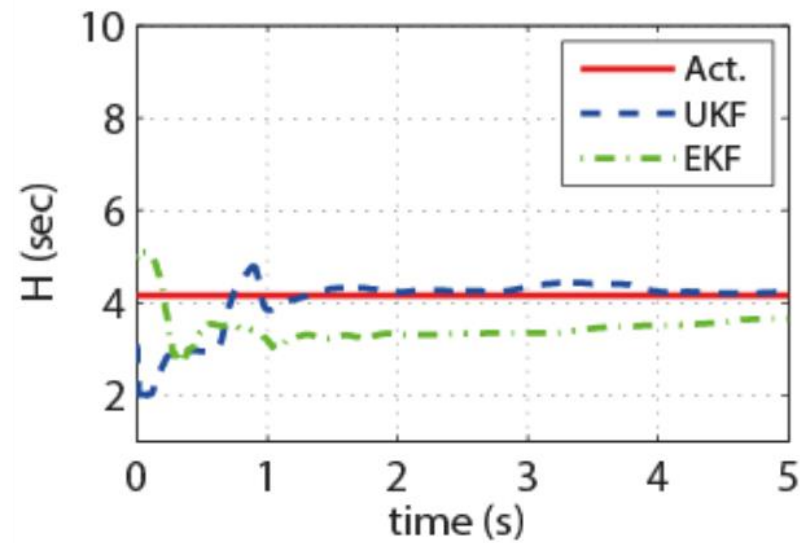
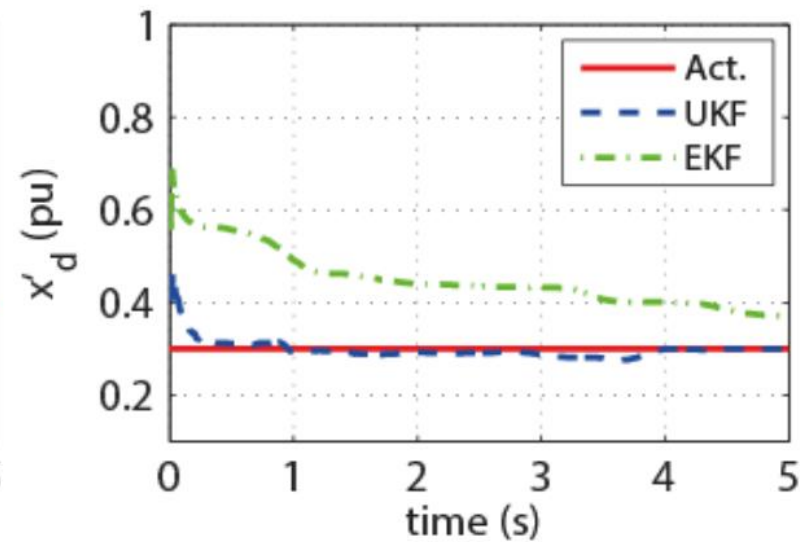
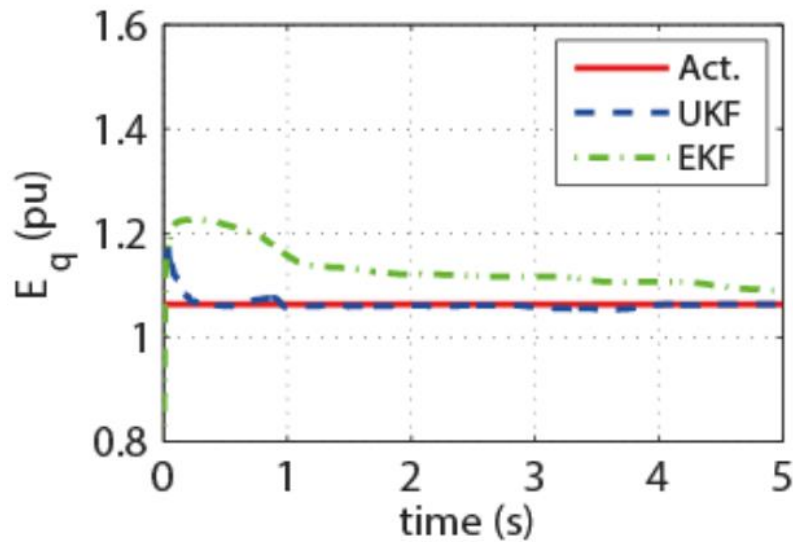
- Concept of pseudo-input used to decouple the model of a generator as observed behind a bus, with V and P as pseudo inputs, and Q and θ as measurements
- Classical model of a generator is used for estimation because parameters are not affected by the subtransient dynamics
- The three parameters are treated as states, with dynamics given by $\frac{dH}{dt} = 0$, $\frac{dx'_d}{dt} = 0$, and $\frac{dE_q}{dt} = 0$, and the complete state vector given by $[\delta_i \ \omega_i \ H_i \ x'_{di} \ E_{qi}]^T$
- The algorithms of UKF and bad-data detection are applied on this decoupled model as before

Test system and measurements

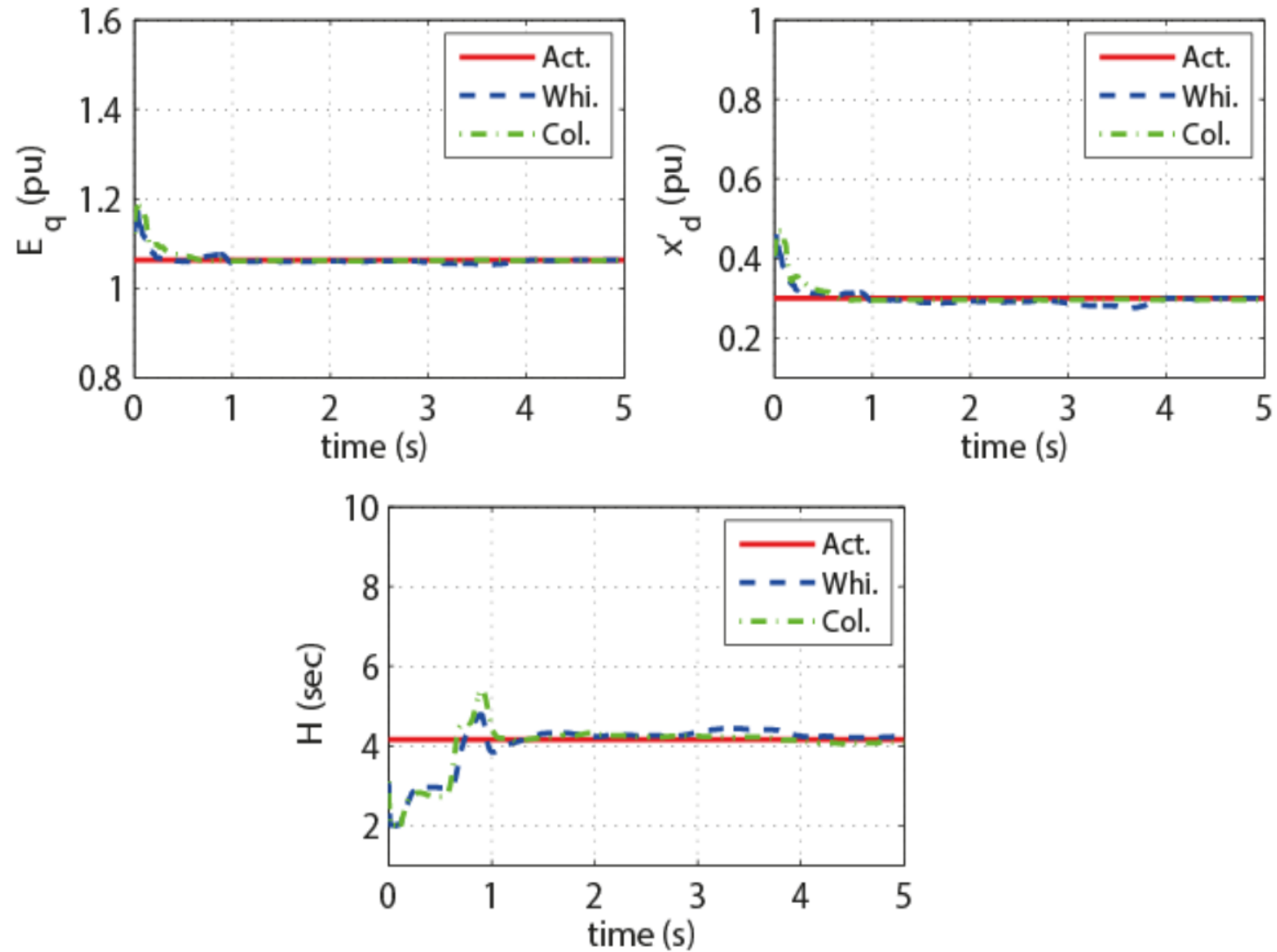
- 16-machine 68-bus benchmark test system used
- Total vector error (TVE) in the measurements is taken as 1%



Results: Comparison with EKF



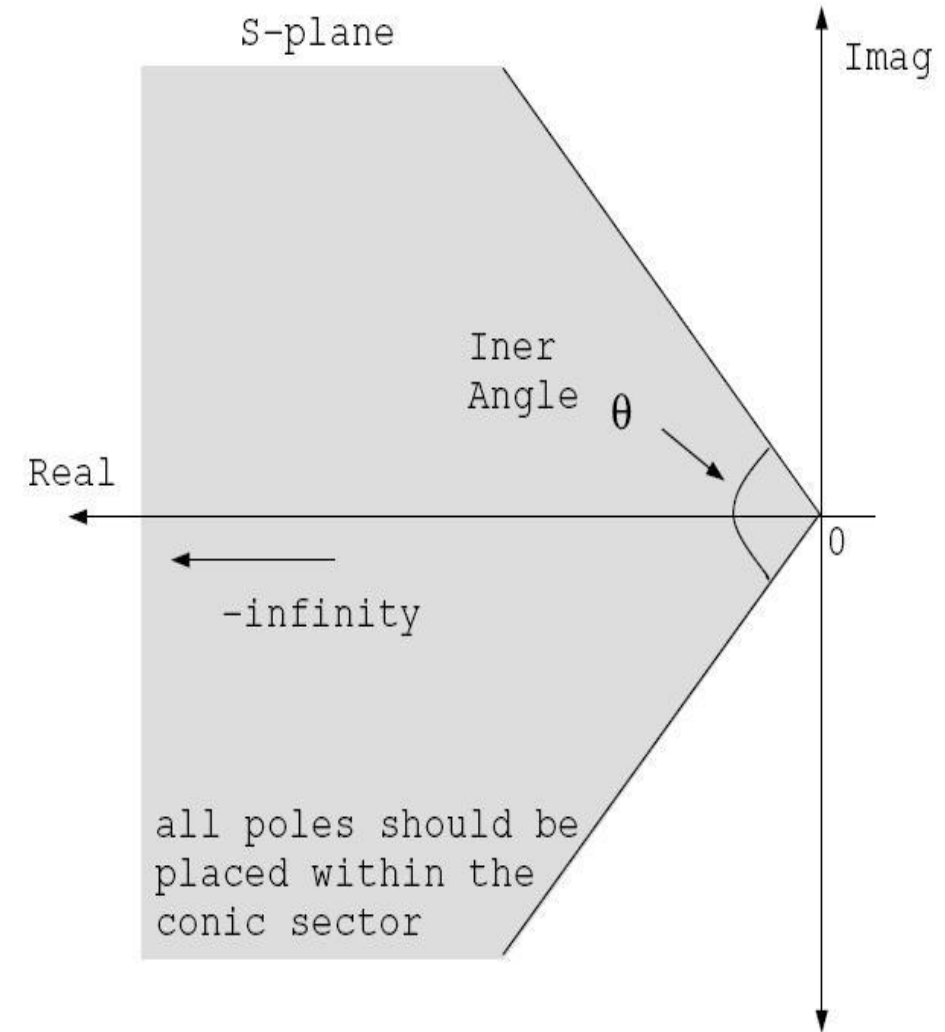
Results: Performance in colored noise



Control based on DSE

Basics of power system oscillatory stability

- After any small or large disturbance in a power system, oscillations occur in system dynamic states (such as rotor speed) or algebraic quantities (such as node voltage or current) – these oscillations are called power system oscillations
- To ensure system stability, any oscillations in the system should be damped-out quickly, otherwise the synchronous machines in the system can move out of synchronism, leading to partial system shutdown or worse – a system-wide black-out
- The eigen values which contribute to power system oscillations are the electromechanical modes – these modes should be confined in a conic section in the left half of eigen-plane for adequate damping



Centralized dynamic estimation and control

- In centralized framework of dynamic estimation and control, remote signals from all over the network need to be brought to a central location
- But centralized framework is not very practical
 - Measurement update rates need to be in ms scale
 - Data loss, time delay, cyber-security threats
 - Complete system model needs to be known
- **Solution**- Decentralization is the most logical solution to the problems of centralized estimation and control as it essentially eliminates most of these problems

Decentralized optimal control based on dynamic state estimation

- Control design should ensure power system oscillatory stability against any disturbance in the system
- Optimal control law needs to be found so that costs associated with state deviations and control efforts are minimized – that is, to achieve control with minimum system changes
- Linear optimal control theory can be used for small disturbances
- Linear quadratic regulator can not be used directly as pseudo inputs are present in decentralized equations
- An optimal control law needs to be derived which incorporates costs associated with pseudo inputs

Decentralization and ELQR methodology

- The decoupled equations of a power system are discretized and linearized:

$$\mathbf{x}_{i(k+1)} = \mathbf{A}_i \mathbf{x}_{ik} + \mathbf{B}_i \mathbf{u}_{ik} + \mathbf{B}'_i \mathbf{u}'_{ik};$$

- Total quadratic cost after incorporating costs associated with pseudo inputs (\mathbf{u}'_{ik}) is $J = \sum_{k=0}^{N-1} [\mathbf{x}_k^T \mathbf{Q} \mathbf{x}_k + \mathbf{u}_k^T \mathbf{R} \mathbf{u}_k + \mathbf{u}'_k{}^T \mathbf{R}' \mathbf{u}'_k]$
- An optimal control law is found which minimizes the total quadratic cost J :

$$\mathbf{u}_{ik} = -(\mathbf{F}_i \mathbf{x}_{ik} + \mathbf{G}_i \mathbf{u}'_{ik}); \quad \mathbf{F}_i = (\mathbf{R}_i + \mathbf{B}_i^T \mathbf{P}_i \mathbf{B}_i)^{-1} \mathbf{B}_i^T \mathbf{P}_i \mathbf{A}_i$$

$$\mathbf{P}_i = \mathbf{Q}_i + \mathbf{A}_i^T \left[\mathbf{P}_i - \mathbf{P}_i \mathbf{B}_i (\mathbf{R}_i + \mathbf{B}_i^T \mathbf{P}_i \mathbf{B}_i)^{-1} \mathbf{B}_i^T \mathbf{P}_i \right] \mathbf{A}_i$$

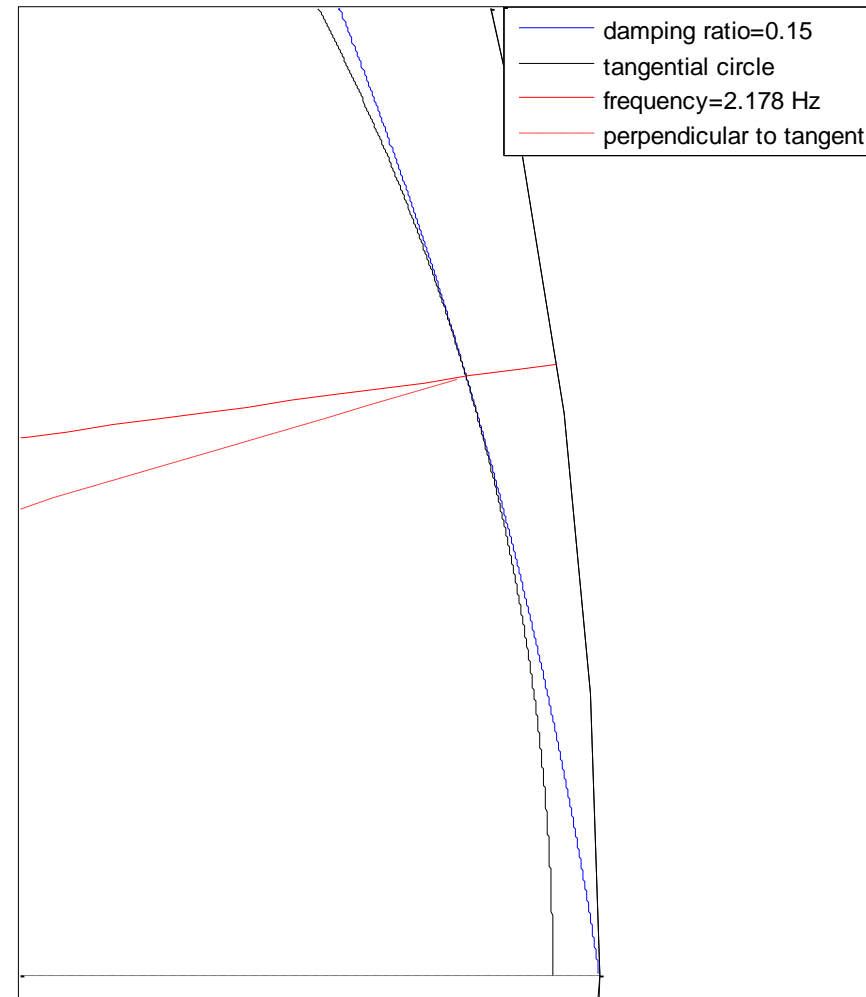
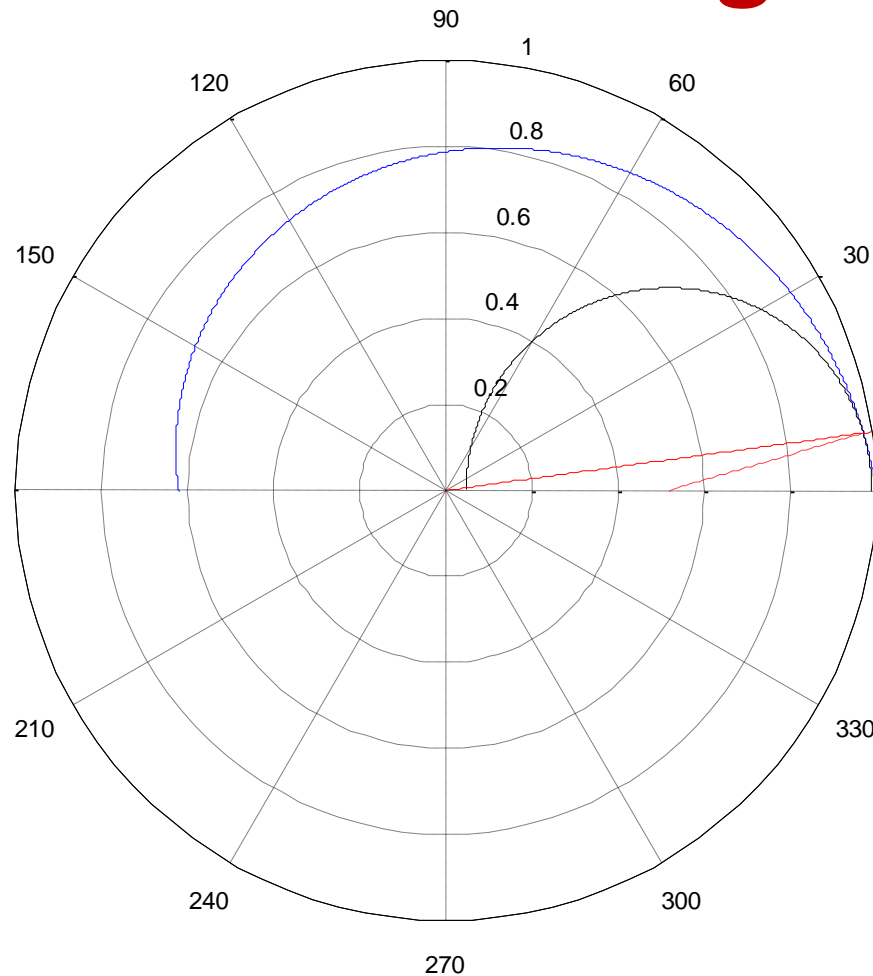
$$\mathbf{G}_i = \mathbf{F}_i \left(\mathbf{A}_i - \mathbf{P}_i^{-1} (\mathbf{P}_i - \mathbf{Q}_i) \right)^{-1} \mathbf{B}'_i$$

- Above control law, named extended linear quadratic regulator (ELQR), implemented at each machine using dynamic estimation of states

Damping control using ELQR

- Conic section corresponding to a specified damping in s-plane maps to a logarithmic spiral in z-plane
- Confining closed loop poles within a spiral is not practical. Hence spiral substituted with a disk of radius r and center $(\beta, 0)$
- The substituting disk should be tangential to the spiral at only one point which corresponds to (f_m, d_{min}) , where f_m is the frequency of the electromechanical pole and d_{min} is the desired minimum damping
- The optimal control law for confining closed loop poles inside this disk remains same as ELQR, except that A, B and B' are replaced by $(A - \beta I)/r, B/r$ and B'/r , respectively.

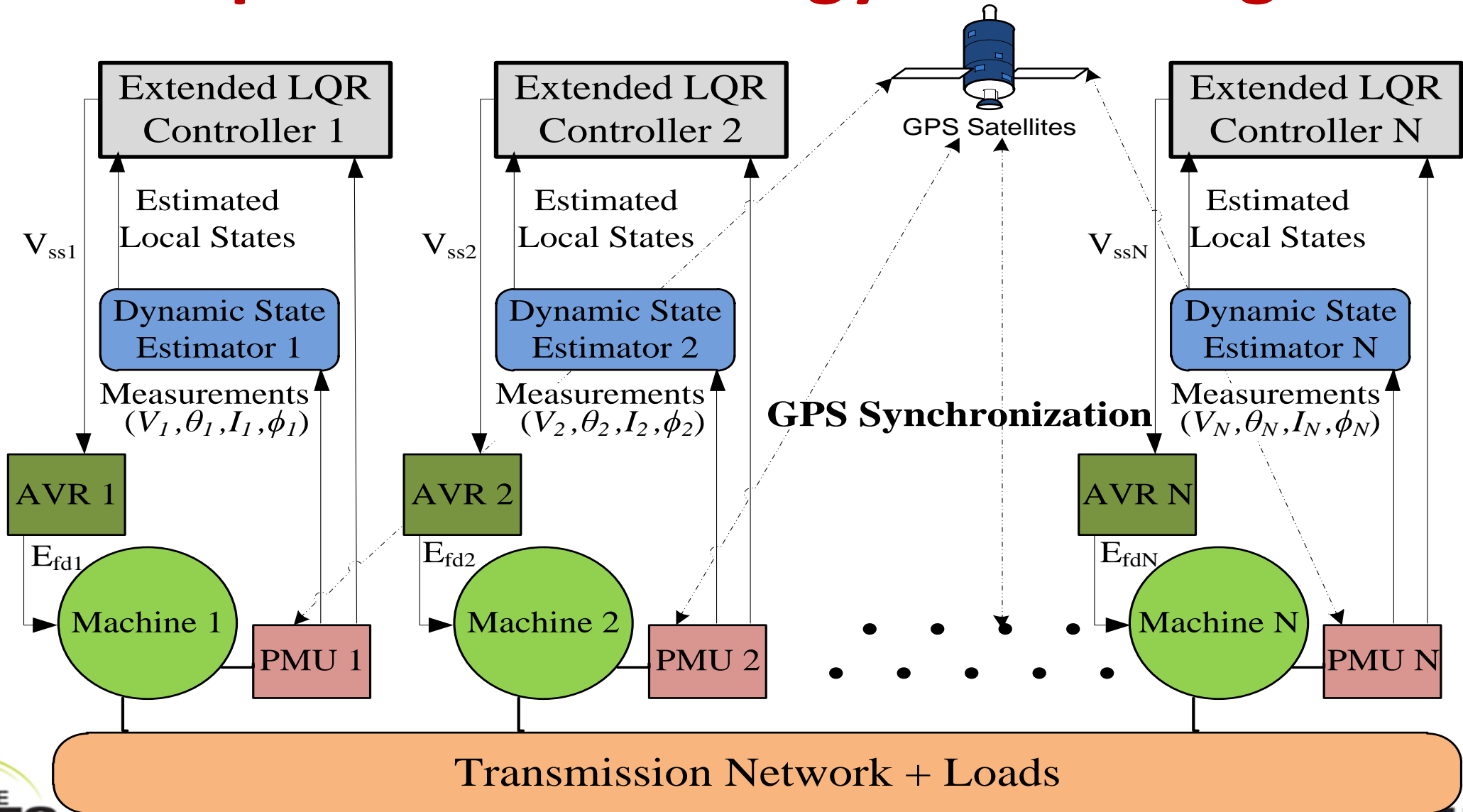
Example: Substituting spiral with a disk– for the 1st generating unit



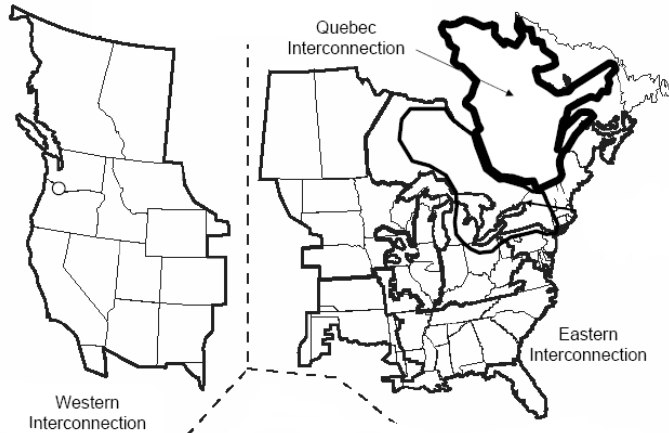
Complete methodology

- Decentralized DSE provides dynamic states at the operating point
- Decoupled equations of a machine (with pseudo-inputs) are discretized and linearized at the operating point using the dynamic state estimates
- Parameters r and β found for the substituting circle after finding the machine's electromechanical poles
- ELQR control gains calculated after incorporating r and β , multiplied with states and pseudo-inputs, and the resulting control applied to the local AVR

Complete methodology: Block diagram

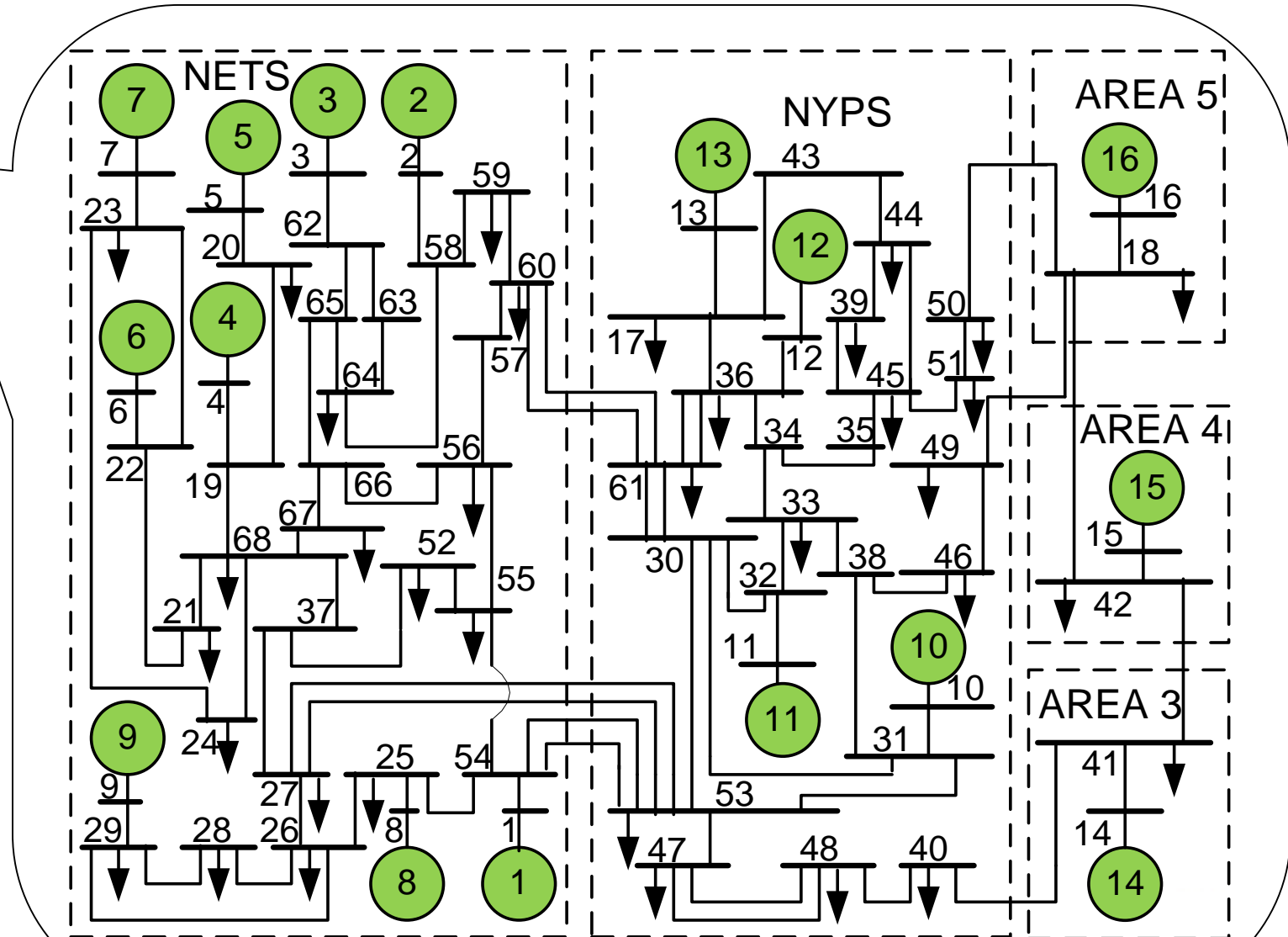


Test system: 68-bus IEEE benchmark model

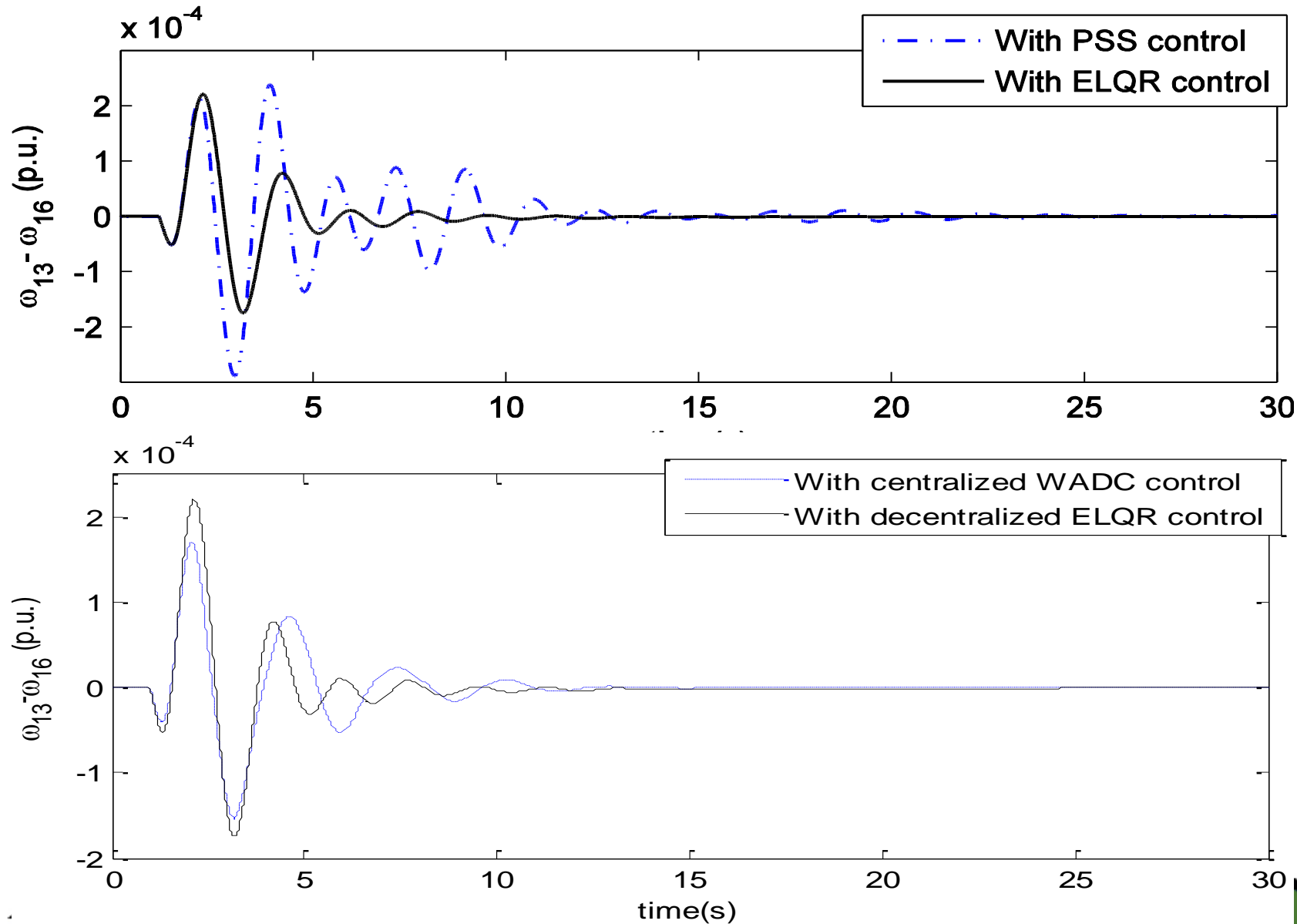


New York & New England inter connected test system

- 16 Machine
- 68 Transmission Bus
- 5 Area
- 1 TCSC



ELQR vs PSS & Wide Area Damping Control



Modal Analysis

	Mode 1		Mode 2		Mode 3		Mode 4	
	Frequency (HZ)	Damping ratio (%)	Frequency (HZ)	Damping ratio (%)	Frequency (HZ)	Damping ratio (%)	Frequency (HZ)	Damping ratio (%)
Open-loop	0.39	2.1	0.52	2.7	0.60	1.9	0.79	4.8
With ELQR	0.31	20.8	0.47	10.6	0.54	11.8	0.76	10.4
With PSS	0.44	14.8	0.54	7.1	0.63	6.9	0.81	7.0
With WADC	0.41	17.8	0.53	12.7	0.67	14.4	0.82	12.5

Quadratic costs

Operating condition: interarea flow and faulted line	Total cost (state-cost+ control-cost) for ELQR control (p.u.)	Total cost (state-cost+ control-cost) for PSS control (p.u.)	Total cost (state-cost+ control-cost) for WADC control (p.u.)
700 MW, 53-54	1.40 (1.16 + 0.24)	1.87 (1.59 + 0.28)	2.15 (2.02 + 0.13)
100 MW, 53-54	0.18 (0.14 + 0.04)	0.30 (0.26 + 0.04)	0.31 (0.29 + 0.02)
900 MW, 53-54	2.46 (2.08 + 0.38)	3.11 (2.69 + 0.42)	3.70 (3.47 + 0.23)
700 MW, 27-53	0.15 (0.13 + 0.02)	0.17 (0.16 + 0.01)	0.23 (0.22 + 0.01)
100 MW, 27-53	0.08 (0.07 + 0.01)	0.12 (0.11 + 0.01)	0.15 (0.15 + 0.003)
900 MW, 27-53	0.18 (0.16+ 0.02)	0.20 (0.19 + 0.01)	0.26 (0.25 + 0.01)

Some limitations

- Useful only for small disturbances – small signal stability
- No mathematical proof or guarantee for global asymptotic stability as only local modes are observed and controlled; more or less works like an adaptive and intelligent PSS which adapts with time to system operating state

One possible solution- Decentralized nonlinear control.

Nonlinear control

- Nonlinear control methods can be broadly divided into two types: methods based on normal forms (or feedback linearization) and methods based on Lyapunov functions (or energy functions)
- In methods based on normal forms, the dynamics of the system are transformed into a new form called as a normal form
- In Lyapunov function based methods, a scalar energy-like function of the system states is found (called as Lyapunov function)
- An advantage of normal form based methods over Lyapunov based methods is that a general technique does not exist for finding a Lyapunov function for a system, while the steps for finding a normal form are well established. Moreover, as a normal form is either fully or partially linear, linear control techniques can be used for the linear part of the normal form

Normal form based control design

- Linearized dynamics (or external dynamics)

$$\begin{aligned} \Delta\delta^i &= z_1^i \\ \Delta\omega^i &= z_2^i \\ \Delta\dot{\omega}^i &= z_3^i \end{aligned} \quad \Delta\ddot{\omega}^i = v_i \quad \begin{bmatrix} \dot{z}_1^i \\ \dot{z}_2^i \\ \dot{z}_3^i \end{bmatrix} = \begin{bmatrix} 0 & 1 & 0 \\ 0 & 0 & 1 \\ 0 & 0 & 0 \end{bmatrix} \begin{bmatrix} z_1^i \\ z_2^i \\ z_3^i \end{bmatrix} + \begin{bmatrix} 0 \\ 0 \\ 1 \end{bmatrix} v_i$$

- Controller expression using LQR theory

$$\begin{aligned} v_i &= -7.0711z_1^i - 13.652z_2^i - 6.1077z_3^i \\ \Rightarrow \Delta\ddot{\omega}^i &= -(7.0711\Delta\delta^i + 13.652\Delta\omega^i + 6.1077\Delta\dot{\omega}^i) \end{aligned}$$

- Representing $\Delta\ddot{\omega}$ in terms of states and inputs

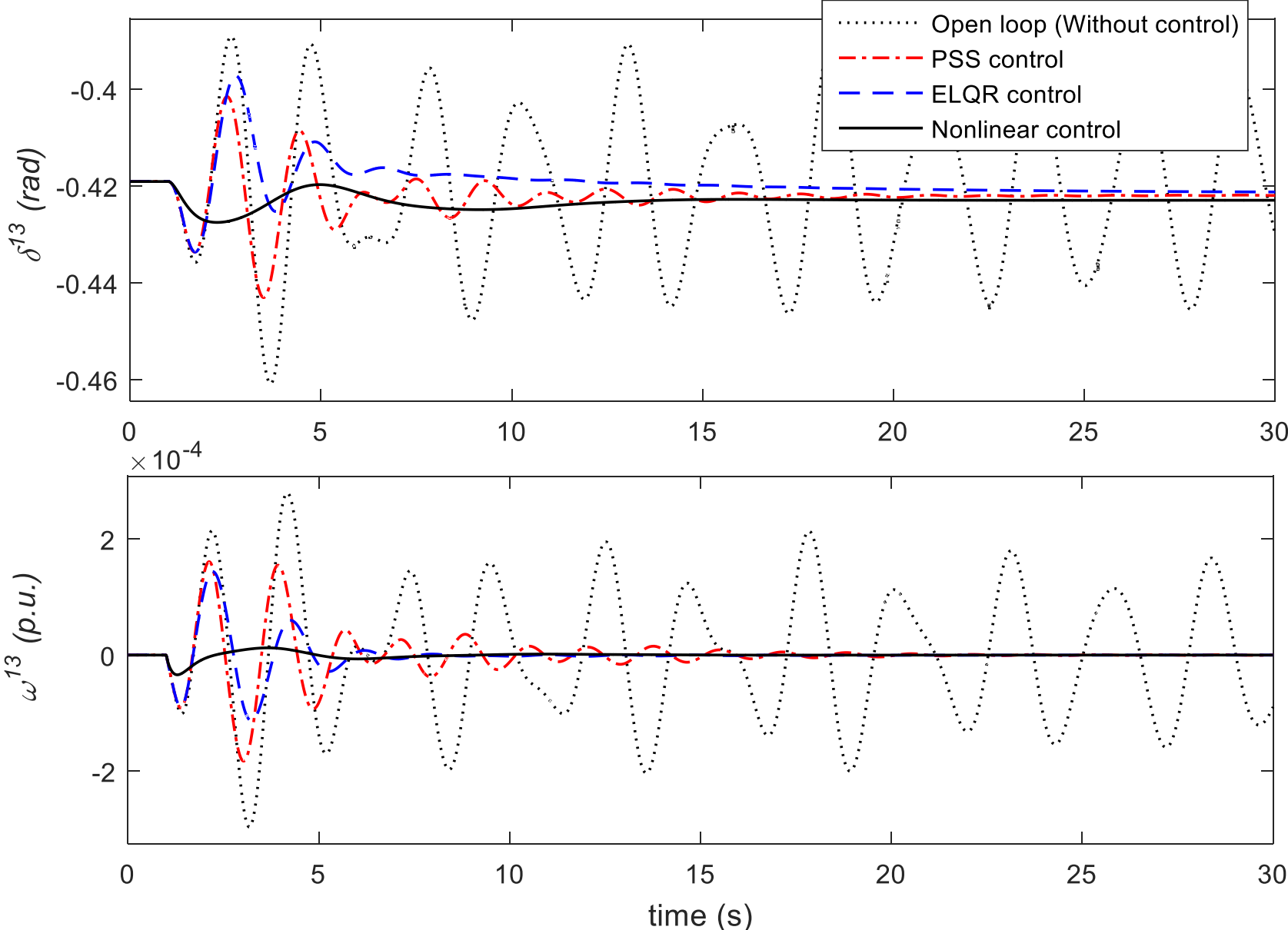
$$\begin{aligned} V_{ss}^i &= \frac{E_{fd}^i}{K_a^i} - V_{ref}^i + V_r^i, \quad E_{fdmin}^i \leq E_{fd}^i \leq E_{fdmax}^i \\ E_{fd}^i &= \frac{T_e^{i'} - [7.07\Delta\delta^i + 13.65\Delta\omega^i + [6.11 - \frac{D^i}{2H^i}]\Delta\dot{\omega}^i] \frac{2H^i}{\omega_0}}{(\omega_0 V_d^i K_{d1}^i) / (\omega^i X_d''^i T_{d0}^i)} - E_q^{i''} \\ E_q^{i''} &= (X_d^i - X_d'^i) [K_{d1}^i I_d^i + K_{d2}^i \frac{\Psi_{1d}^i - E_q'^i}{X_d'^i - X_l^i}] - E_q'^i \end{aligned}$$

Asymptotic stability

- The states which do not appear in external dynamics describe the internal dynamics of the system
- It needs to be shown that both the internal and external dynamics remain stable under the nonlinear control in order to show the stability of a power system
- Global asymptotic stability is rigorously established by the following theorem:

The internal dynamics of a power system will remain asymptotically stable if the external dynamics of all the machines in system are asymptotically stable

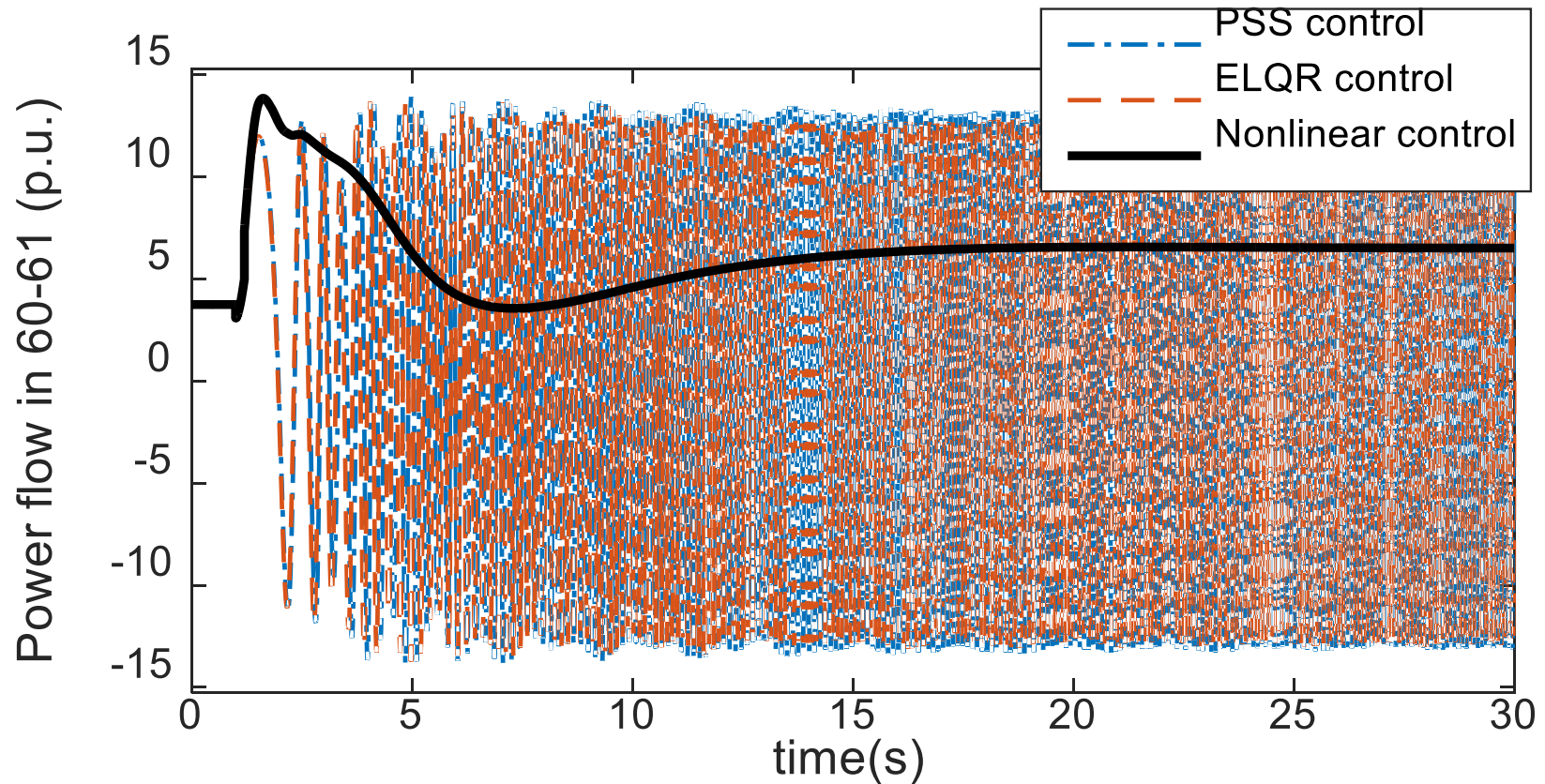
Results for small signal stability



Results for small signal stability – modal analysis

	Open-loop	PSS control	ELQR control	Nonlinear control
Mode-1 frequency (Hz)	0.39	0.43	0.31	0.12
Mode-1 damping ratio (%)	0.9	11.4	18.7	47.2
Mode-2 frequency (Hz)	0.52	0.54	0.47	0.20
Mode-2 damping ratio (%)	2.1	6.3	9.8	92.8
Mode-3 frequency (Hz)	0.60	0.63	0.54	0.21
Mode-3 damping ratio (%)	1.2	5.7	11.0	91.0

Results for transient stability



	PSS control	ELQR control	Nonlinear Control
CCT (ms)	40	50	220

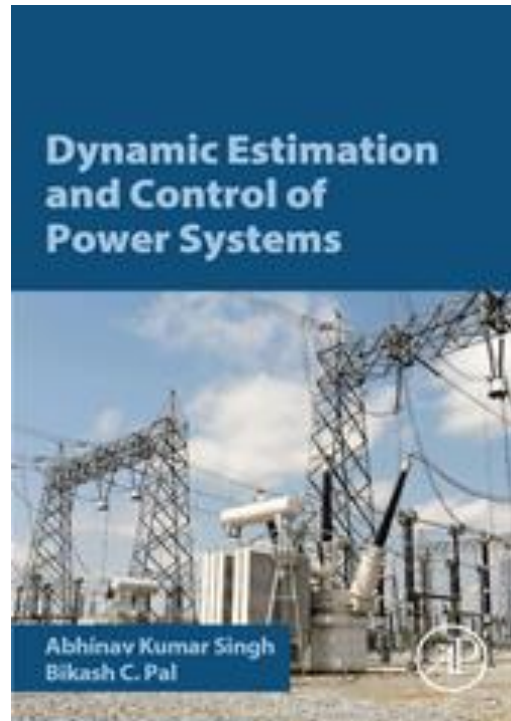
A drawback of non-linear control

- Control costs are very high as compared to linear control methods – around 10 times higher for the case study

Solution - It is best to use both linear and non-linear control in a complementary manner – use linear control methods for small disturbances and in quasi steady state condition, and switch to nonlinear control methods as soon as a large disturbance is detected

Further study

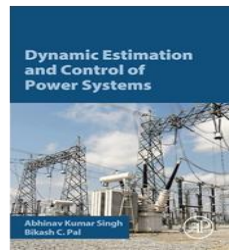
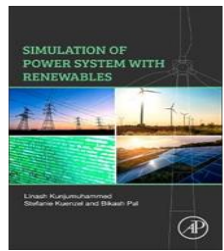
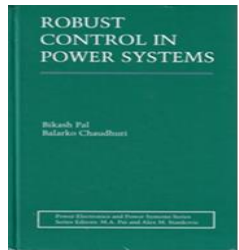
A. K. Singh and B. C. Pal, *Dynamic Estimation and Control of Power Systems*, Academic Press, Cambridge, USA, 2018.



Control



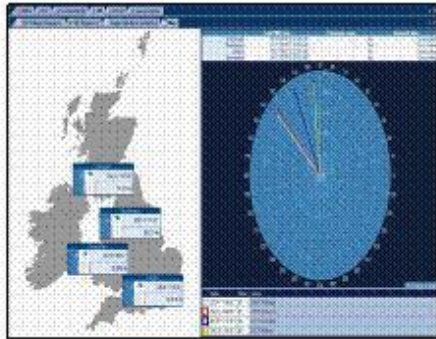
Sowmya



Monitoring



Onyema



Modelling



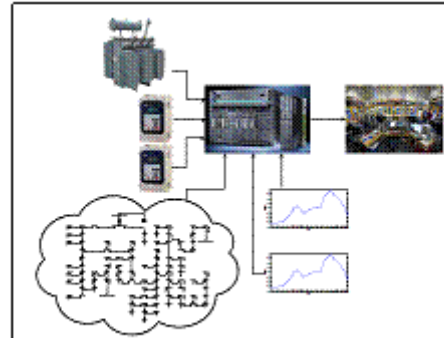
Adeyemi



Estimation



Firdous



Kevin



Diptargha



Magne



Jerome



Abhinav



Stratis



Nicolas

Our funding supports



European
Research
Council



Questions?